UC Berkeley
UCCONNECT

Title
Control Strategies for Corridor Management

Permalink
https://escholarship.org/uc/item/1dk6b1dg

Authors
Amiri, Zahra
Lo, Yu-Chieh
Skabardonis, Alexander
et al.

Publication Date
2016-06-28

UCONNECT

Control Strategies for Corridor Management

Final Report UCCONNECT 2016 - TO 008 - 65A0529

Zahra Amiri; Graduate Student; University of California, Berkeley
Yu-Chieh Lo; Graduate Student; University of California, Berkeley
Alexander Skabardonis; Professor; University of California, Berkeley
Pravin Varaiya; Professor; University of California, Berkeley

2016

Berkeley   UC Irvine   UCLA   UCR   UCSB   CAL POLY POMONA

STATE OF CALIFORNIA • DEPARTMENT OF TRANSPORTATION
TECHNICAL REPORT DOCUMENTATION PAGE
TR0003 (REV 10/98)

1. REPORT NUMBER	2. GOVERNMENT ASSOCIATION NUMBER	3. RECIPIENT'S CATALOG NUMBER
2016 – TO 008 – 65A0529		

4. TITLE AND SUBTITLE	5. REPORT DATE
Control Strategies for Corridor Management	6/28/16
	6. PERFORMING ORGANIZATION CODE
	N/A

7. AUTHOR	8. PERFORMING ORGANIZATION REPORT NO.
, Zahra Amiri, Yu-Chieh Lo, Alexander Skabardonis, Pravin Varaiya	N/A

9. PERFORMING ORGANIZATION NAME AND ADDRESS	10. WORK UNIT NUMBER
University of California at Berkeley Institute of Transportation Studies Berkeley, CA 94720	N/A
	11. CONTRACT OR GRANT NUMBER
	65A0529

12. SPONSORING AGENCY AND ADDRESS	13. TYPE OF REPORT AND PERIOD COVERED
California Department of Transportation (Caltrans) 1227 O Street Sacramento, CA 95814 University of California Center on Economic Competitiveness in Transportation (UCCONNECT) 2616 Dwight Way, Berkeley, CA 94720-1782	Final Report, 3/1/15 – 2/29/16
	14. SPONSORING AGENCY CODE
	N/A

15. SUPPLEMENTARY NOTES

16. ABSTRACT

Integrated management of travel corridors comprising of freeways and adjacent arterial streets can potentially improve the performance of the highway facilities. However, several research gaps exist in data collection and performance measurement, analysis tools and control strategies. In this project first we analyzed high resolution data consisting of time-stamped records of every event involving vehicles, together with the signal phase at real-world signalized intersections and developed procedures for estimating performance measures. Next, we assessed the performance of a new microscopic simulator for signalized arterials. The model predictions were in close agreement with the predictions from widely used models in practice. We also developed and applied control strategies for freeway-arterial coordinated control to avoid queue override and developed a methodology to provide estimates of the amount and impacts of freeway diverted traffic in case of no-recurrent (incident related) congestion.

17. KEY WORDS	18. DISTRIBUTION STATEMENT
Traffic signals, mathematical models, freeway control, simulation	No Restriction.

19. SECURITY CLASSIFICATION (of this report)	20. NUMBER OF PAGES	21. COST OF REPORT CHARGED
Unclassified		

Reproduction of completed page authorized.

ABSTRACT

Integrated management of travel corridors comprising of freeways and adjacent arterial streets can potentially improve the performance of the highway facilities. However, several research gaps exist in data collection and performance measurement, analysis tools and control strategies. In this project first we analyzed high resolution data consisting of time-stamped records of every event involving vehicles, together with the signal phase at real-world signalized intersections and developed procedures for estimating performance measures. Next, we assessed the performance of a new microscopic simulator for signalized arterials. The model predictions were in close agreement with the predictions from widely used models in practice. We also developed and applied control strategies for freeway-arterial coordinated control to avoid queue override and developed a methodology to provide estimates of the amount and impacts of freeway diverted traffic in case of no-recurrent (incident related) congestion.

Keywords:

Traffic signals, mathematical models, freeway control, simulation

ACKNOWLEDGEMENTS

TABLE OF CONTENTS

LIST OF FIGURES

LIST OF TABLES

CHAPTER 1

INTRODUCTION

1.1 Problem Statement

Considerable attention has been given to new approaches for improving the transportation system because of limited funding and environmental concerns for constructing new highway facilities. One promising approach is implementation of advanced signal control strategies along arterials. This would reduce unnecessary delays and stops at traffic signals, improve travel times and cut fuel consumption and emissions. In many instances these arterial facilities also serve as reliever routes for congested freeways especially under incident conditions. Thus their efficient operation could be significant for the traffic performance along the entire travel corridors.

Recent assessment of the state of practice in signal management on urban networks indicates that on average our intersections are poorly managed, according to the National Transportation Operations Coalition (NTOC) 2012 signal systems report card [1]. The main reason for the poor performance is the lack of systematic data collection to estimate performance measures and the development and implementation of control strategies that are responsive to real-time changes to traffic patterns and at the same time are simple and effective. Several adaptive control strategies have been developed but their implementation is limited because of the complexity and the extensive and costly data requirements [2]. Freeway-arterial coordination concepts have also been proposed but their practical implementation is quite limited because of data limitations, modeling challenges and institutional issues.

Recent advances in technology are making high resolution (HR) data collection at traffic signals economical [3,4]. Furthermore, these data can be complemented by measurements of aggregate performance, such as travel times and origin-destination patterns, derived from vehicle-based records of GPS traces or Bluetooth and WiFi addresses [5]. Together, these data present a game-changing opportunity in traffic management.

1.2 Project Objectives

The research described in this report is concerned with the analysis of HR data to calculate performance measures at traffic signals, and use these data to develop improved control algorithms and improved freeway-arterial coordination strategies. The methodology consists of empirical data collection and analysis, analytical modeling, and simulation testing. It builds on recent and ongoing work by the research team on algorithms for estimating performance measures based on HR and emerging data sources development of testing of strategies for traffic signal control and freeway-arterial coordination [5,6,7,8]. The objectives of the research project are:

- Collect and analyze high-resolution (HR) data at signalized intersections. Develop and apply procedures for calculating performance measures, and developing improved signal plans.
- Application and evaluation of emerging analysis tools for signalized arterials.
- Propose and test freeway-arterial coordination strategies for preventing queue override on metered ramps, and accommodating freeway diverted traffic on arterials under incident conditions.

1.3 Organization of the Report

This document is the final report for the project. It describes in detail the work performed and presents the study findings. Chapter 2 describes the test site for collecting and processing HR data, and the estimation of the performance measures. The evaluation of the PointQ simulation model is Chapter 3. The development and simulation testing of freeway-arterial coordination strategies are presented in Chapter 4. Chapter 5 summarizes the study findings and outlines future research directions. Appendix A includes the study database. Appendix B includes a research paper produced from the project, on queue length estimation at signalized intersections based on HR data.

CHAPTER 2

PERFORMANCE MEASURES BASED ON HIGH RESOLUTION (HR) DATA

2.1 Performance Measures at Traffic Signals

The purpose of this Chapter is to present the acquisition and analysis of HR data to obtain measures of effectiveness (MOEs) for the development and evaluation of connected vehicle based traffic signal control strategies.

Several MOEs have been proposed and used for evaluating traffic operations at highway facilities controlled by traffic signals. Table 2.1 displays MOEs most commonly proposed for the development and evaluation of traffic signal control algorithms. These MOEs vary depending on the operating environments (isolated intersections, arterials, grid networks), traffic conditions and patterns (e.g., congested-undersaturated vs. oversaturated conditions) and objectives/constraints (mobility, safety, environment). Field data collection of most of these MOEs with conventional approaches is expensive and time consuming, which limits the collection of data only when major design or control improvements are implemented, and does not allow for systematic monitoring of traffic performance.

In addition to the MOEs in Table 2.1, the following indicators of performance are commonly used to assess the quality of traffic operations at highway facilities:

- Level of Service (LOS) per the Highway Capacity Manual (HCM) [10]
- Volume/Capacity ratio (v/c)

Level of service (LOS) is a quality measure describing operational conditions within a traffic stream, generally in terms of such service measures as delay, freedom to maneuver, traffic interruptions, and comfort & convenience. Six LOS are defined for each type of facility that has analysis procedures available; LOS A represents the best operating conditions, and LOS F the worst. The average delay (sec/veh) is used to characterize the LOS at signalized intersections. Table 2.2 shows the relationship between the average delay per vehicle and the LOS.

Table 2.2 LOS table from Highway Capacity Manual [10]

Control Delay (s/veh)	LOS by Volume-to-Capacity Ratio[a]	
	≤1.0	>1.0
≤10	A	F
>10–20	B	F
>20–35	C	F
>35–55	D	F
>55–80	E	F
>80	F	F

Note: [a] For approach-based and intersectionwide assessments, LOS is defined solely by control delay.

The (v/c) ratio indicates the level of congestion at an intersection approach or the entire intersection; v/c ratios greater than 1.00 indicate that the traffic demand is higher than capacity which results in oversaturated conditions with long delays, and excessive queue lengths, and cycle failures.

Table 2.1 Performance Measures for Signal Systems [9]

I. MOBILITY

Operating Environment	Operating Conditions	Performance Measure	Units	Comments
Intersection	Undersaturated	Average control delay	sec/veh	Difference free-flow travel time and actual travel time
		Max back of queue	#veh (ft/l)	Average and 95th % of the max extend of queue throughout the cycle
		Cycle failure	%	Proportion of cycles that queue failed to clear during green
		Green time utilization	%	Proportion of green utilized by traffic demand served by the phase
	Oversaturated	Throughput	#	# vehicles served at the intersection per time interval
Arterial/ Grid Network	Undersaturated	Average travel time	(min)	Average travel time for movements served by coordinated signal phases
		Average travel speed	(mph)	Average travel speed for movements served by coordinated signal phases
		Travel time variability	(min)	st deviation, 80th or 95th percentile of travel times served by coordinated phases
		# of stops/stop rate	#/(%)	Average # of stops (fraction of veh stopped) for movements served by coordinated phases
		Total delay	veh-hr	Delay of all vehicles served in the system
		% vehicles in the green	%	Proportion of platoon arriving during the green time per signal cycle
		Bandwidth efficiency	%	Proportion of the green through bandwidth to the signal cycle
		Attainability	%	Proportion of green bandwith to the min green time for the through phase
		Transit delay[1]	sec/bus	average delay to transit vehicles at traffic signals
		Acceleration noise	ft/sec²	Standard deviation of veh accelerations
	Oversaturated	Throughput	#	# veh served
		Extend of queue	#/mi	Distance or # of street segments with queue spillback
		Congestion duration	hr	Duration of oversaturated conditions

II. SAFETY

Operating Environment	Operating Conditions	Performance Measure	Units	Comments
Intersection/ Arterial/ Grid Network	Undersaturated/ Oversaturated	# accidents per type	#/yr	# of accidents by severity and/or traffic movement (e.g., # left turn related accidents)
		Encroachment time (ET)	# conflicts	Surrogate conflict measure
		# RLR	#	# of red light running violators
		# vehicles in yellow	#/cycle	# vehicles in platoon arrive in the yellow clearance interval per signal cycle

III. ENVIRONMENTAL

Operating Environment	Operating Conditions	Performance Measure	Units	Comments
Intersection/ Arterial/ Grid Network	Undersaturated/ Oversaturated	Fuel Consumption	gal	Excess fuel consumption due to delay & stops
		HC/CO/NOx/CO2/PM	/gr/m,	Air pollutant emissions / concentrations
		Noise	[db]	Inceased noise level due to congestion

2.2 HR System

High resolution (HR) data at signalized intersections refers to the continuous acquisition of detector data that provide information on the vehicles approaching and leaving the intersection plus simultaneous information on the signal status (signal display). In this research we are utilizing the SAMS (Safety and Mobility System) originally developed and field implemented by Sensys Networks Inc. [6].

Figure 2.1 shows the schematic of the detector layout for a signalized intersection in the city of Danville, CA, equipped with SAMS. Each approach has stop bar detectors denoted by grey circles, and an advance detector (not shown). In addition there is a detector in each departure lane, denoted by red circles, which permits measurement of turn movements. There is a

network monitoring card that provides the signal phase. The vehicle detectors are magnetometers that send the detection events wirelessly to the Access Point (AP). The AP also receives the signal phase events. The AP time stamps all events with an accuracy of 10ms. The event stream is sent via a cellular modem to a server. The intersection is also equipped with a PTZ camera, which allows to verify the accuracy of the data collection process.
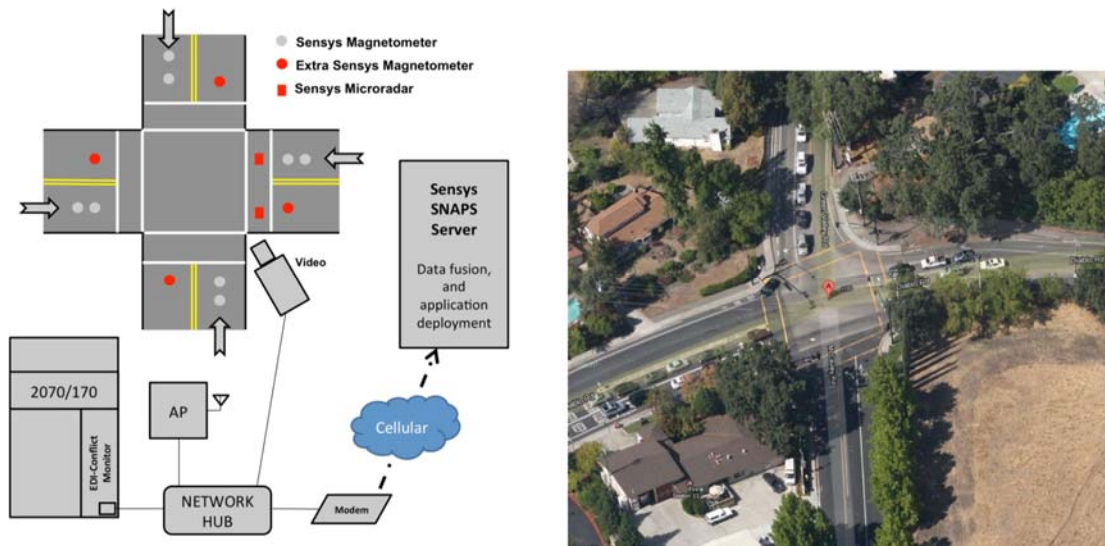
Figure 2.1 Sample SAMS Instrumented Intersection, Danville CA

2.3 The Selected Test Site and HR Database

The selected test site is a signalized intersection in Beaufort, SC (Figure 2.2). The Intersection has four approaches (legs) and there are three movements per approach. As is shown in Figure 2.2, the sensor instrumentation includes upstream detectors on each travel lane located approximately 200 to 300 ft upstream from the stop-line, stop bar detectors. Also, departure lane detectors are located on each lane downstream of the stop-line. The signal phasing and timing information are shown in Figure 2.2(b). There are leading left-turn phases on the main road (legs 1&3) and split phasing on the cross streets. The signal operates as coordinated traffic actuated with fixed-time of day timing plans. There are a total of nine fixed-time timing plans for AM, midday and PM peak on weekdays plus weekends, light traffic and saturated conditions.

The HR data available consist of detector recordings at each detector as each vehicle enters and leaves the intersection along with signal phase and timing information. The data are processed and stored into different sets on a server at various time resolutions (Appendix A includes a list of the data):
- Data set 1: turning movement counts, delay, signal phase duration
- Data set 2: Saturation flows for each lane
- Data set 3: signal settings per cycle (green time, wasted green time, cycle length)
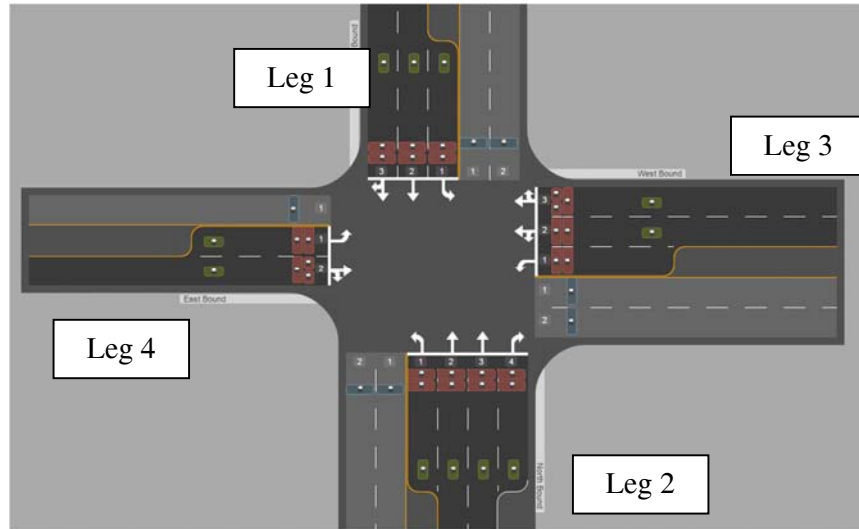
(a) Intersection Geometrics
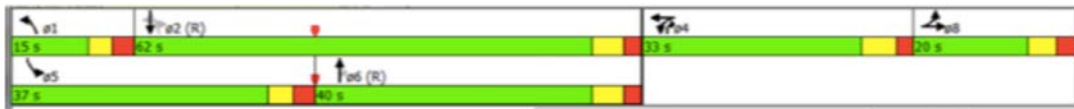
Time Period/Phase	1	2	3	4	5	6	7	8	Cycle Length
AM Peak (6AM-9AM)	15	40	N/A	39	15	40	N/A	16	110
Mid Day (9AM-2PM)	17	53	N/A	33	25	45	N/A	17	120
PM Peak (2PM-7PM)	15	62	N/A	33	37	40	N/A	20	130

(b) Signal Phase and Timing

Figure 2.2 Test Intersection-Ribaurt Rd@Lady's Island Drive, Beaufort, SC

2.4 Estimation of Performance Measures Using the HR Data

The following sections describe the processing and analysis of the HR data for a typical weekday, Wednesday February 18, 2015 from 6:00 am to 7:00 pm.

2.4.1 Vehicle Counts

The processing of sensor data provides flow rates at user selected time resolution for each movement, approach and the entire intersection. Figure 2.3 shows the total number of vehicles per hour that entered the test intersection. Note that, each bar presents the traffic volume in the past 1 hour, i.e., the value at 7AM bar shows the total traffic volume from 6AM to 7AM. The average total flow is 2,810 vph, and the standard deviation is 594 vph. The maximum number of vehicles that entered the intersection per hour is 3,640 vph at 6:00 PM and the minimum is 1,371 vph, at 6:00 AM. The traffic volume is fairly constant in the AM peak (8-9) and PM peak (4-6), indicating that adaptive control in these time periods may not produce significant benefits compared to fixed time of day plans.
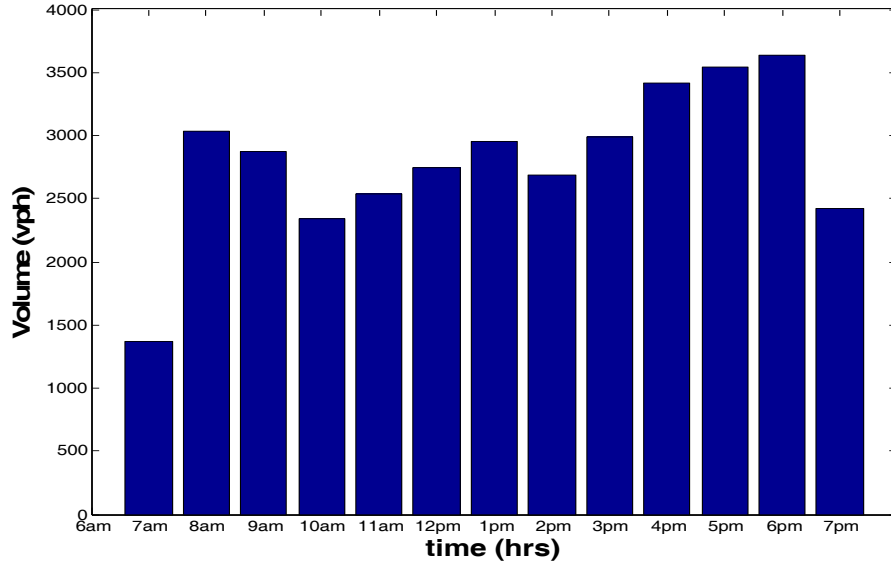
Figure 2.3 Total Intersection Traffic Volume

The vehicle counts per movement are calculated by matching the stop-bar and departure lane detections to determine the turn movement of each vehicle. Figure 2.4 shows the turning movement counts (#veh/15 minutes) for leg 1.
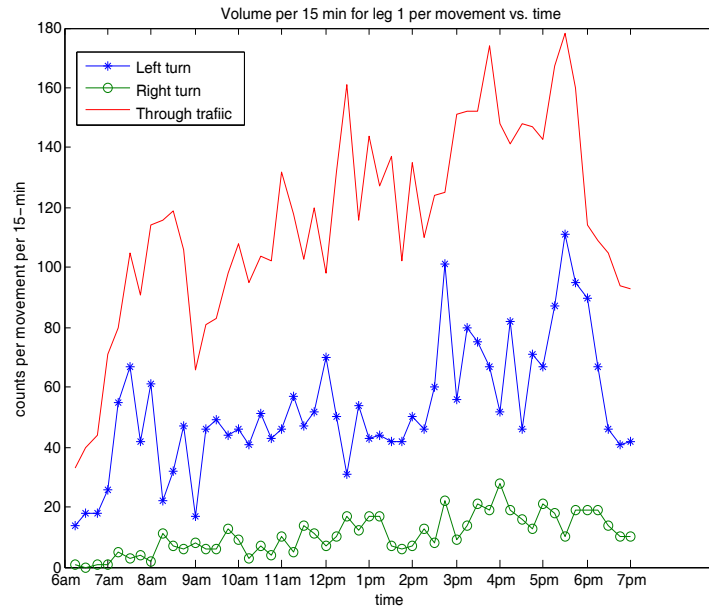
Figure 2.4 Turning Movement Counts--Leg 1 (veh/15min)

2.4.2 Signal timing data

The processing of signal timing data provides the green time per phase and the cycle length. Figure 2.5 shows the cycle length and the green time for the phases serving the left turns and through movements on legs 1 and 2. Phase 2, which serves the through movement in leg 1, has the longest green time. As shown in the Figure, the green time for Phase 6 which serves the through movement in leg 2, is very close to phase 1.
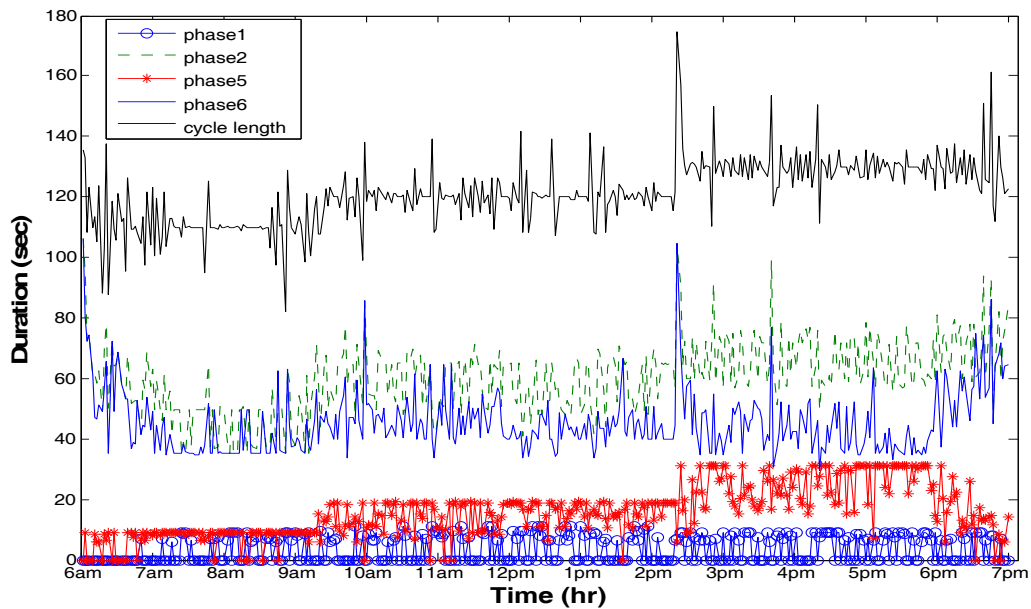
Figure 2.5 Cycle length and Green Times

The signal timing data also provide information about the wasted green time per phase. Wasted green time is the time interval that a particular phase remains green but no vehicles enter the intersection from that movement and there is an active call (request for service) by other phase(s).

Figure 2.6 shows the frequency of the wasted green time for phase 4 (leg 3) during the analysis period (6am-7pm). It can be seen that in over 56% of the signal cycles there is a wasted green time of longer than 4 sec., indicating the need for adjusting the existing signal settings.
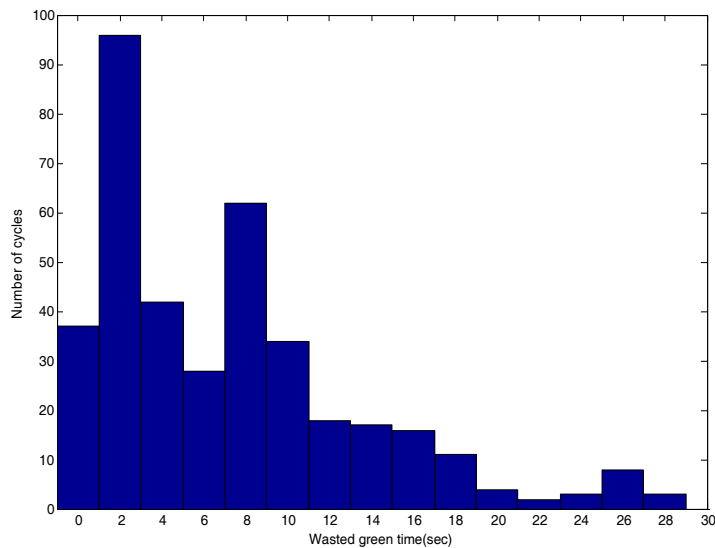
Figure 2.6 Wasted Green Time, Phase 4

8

Figure 2.7 shows the percentage of vehicles arrived on green for through movement of leg 2 (phase 6). These values are calculated by dividing the number of vehicles arrived during the green interval over the total number of vehicles that arrived per cycle. The proportion of arrivals of green is used to assess the quality of signal progression along arterials. The higher percentage of arrivals on green the less number of stops and delay at the intersection approach. A similar widely measure is the Purdue Coordination Diagram (PCD) [3] which shows the vehicle arrivals per cycle relative to the start of the green in the same diagram for a chosen time period. Arrival on green values also can be used to determine the arrival type and the platoon progression factor for estimating signalized intersection delay per the Highway Capacity Manual procedures [10].
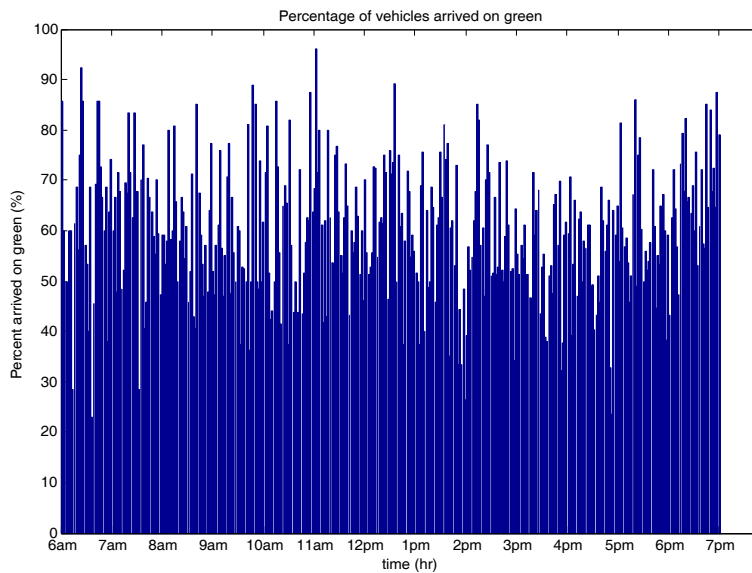
Figure 2.7 Proportion of Vehicles Arriving on Green (%)—Phase 6

2.4.3 Saturation flow, Start-up lost time and Volume/Capacity (v/c) ratio

Saturation flow is the maximum flow rate that can be sustained during the green signal phase, assuming there is a continuous queue present, expressed in vehicles/hour of green (vphg). It is estimated by measuring the time of discharge (i.e. the event-time) between the fourth and eighth queued vehicles at the signalized intersection approach. The first three vehicles in the queue are not used because of the start up lost times. Table 2.3 shows the measured average saturation flow rate for selected intersection approaches.

Table 2.3 Saturation Flow Rates

APPROACH	MOVEMENT	SATURATION FLOW (veh/hr/l/g)
1	THROUGH	1727
	LEFT	1798
2	THROUGH	1728
3	THROUGH	1723
	LEFT	1828
4	THROUGH	2219

The start-up lost time is calculated from the discharge time of the first four vehicles in the queue and the saturation flow as follows:

$$l_s = t_4 - \frac{3600}{S} \times 4 \qquad (2\text{-}1)$$

Where:
l_s: start time lost time (seconds)
t_4: discharge time of the first four vehicles in the queue (seconds)
S: saturation flow (vphg)

The calculated saturation flow is used with the signal timing data to obtain the volume to capacity (v/c) ratio for an intersection approach, and delay. The v/c ratio is calculated as follows:

$$v/c = \frac{v \times C}{g \times s} \qquad (2\text{-}2)$$

Where:
C: cycle length (seconds)
g: the effective green time (actual green time –start-up lost time (seconds)
v: traffic volume (vph)

The v/c ratio is a measure of the level of congestion for a particular movement or approach. (v/c) ratio greater than 1 indicates that the approach is oversaturated, i.e., queues do not clear at the end of the green period. Figure 2.8 shows the estimated v/c ratio for through movement of leg 2, throughout the analysis period based on the vehicle count and signal timing data. As is shown in Figure 2.8 the v/c ratio is less than 0.6 for most of the analysis period, except short times during the peak periods.
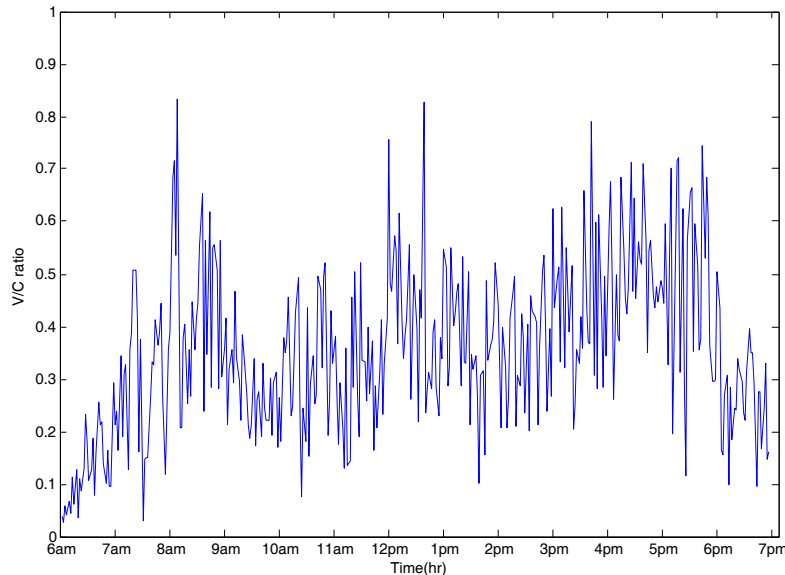
Figure 2.8 Volume/Capacity (v/c) Ratio for Through Movement--Leg 2

Figure 2.9 shows the v/c ratios for all six phases over one day in 15 min intervals for the Danville sample intersection (Figure 2.1). Also shown is the level of service (LOS) based on (v/c) ratio. These plots suggest possible tradeoffs among the green splits between signal phases in order to improve the worst LOS.
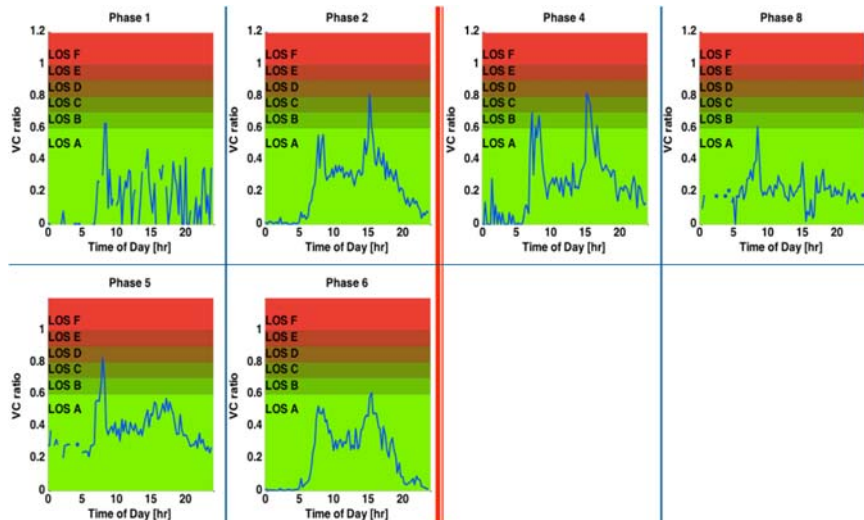
Figure 2.9 V/C and Level of service (LOS)—Danville Intersection

2.4.4 Delay

The delay (waiting time) is calculated as follows: each time a vehicle crosses the advanced detector, its time to join the queue is computed by calculating when the car would get to the stop-bar, traveling at its free-flow speed (assumed as the speed limit). This is done for each car that arrives during a red interval. Once the signal turns green, the queue is assumed to immediately discharge. Thus, the average delay is computed using the time of arrivals of each vehicle to the queue, and the time when the signal turns green. Figure 2.10 shows the average delay per vehicle per cycle for leg 2 through movement.

Figure 2.10 also shows the average delays for the same movement calculated using the analytical formula (2-3) below based on deterministic queuing (first term in the HCM delay estimation equation [10]):

$$d = \frac{C\left(1 - \frac{g}{C}\right)^2}{2(1 - \frac{g}{C} \times \frac{v}{c})}$$

(2-3)

The HR data derived and the analytically determined delays are in reasonably close agreement. The HR data based delays are longer than the analytically estimated values, because the analytical method does not take into consideration the random delays (second term in the HCM signalized intersections delay equation).

Figure 2.11 shows the average delays per phase and the associated LOS according to HCM (Table 2.2). Most of the movements at the intersection have acceptable performance (LOS D or better). However, in phase 8 (leg 4 all the movements) high delay and LOS F occur in several time intervals.
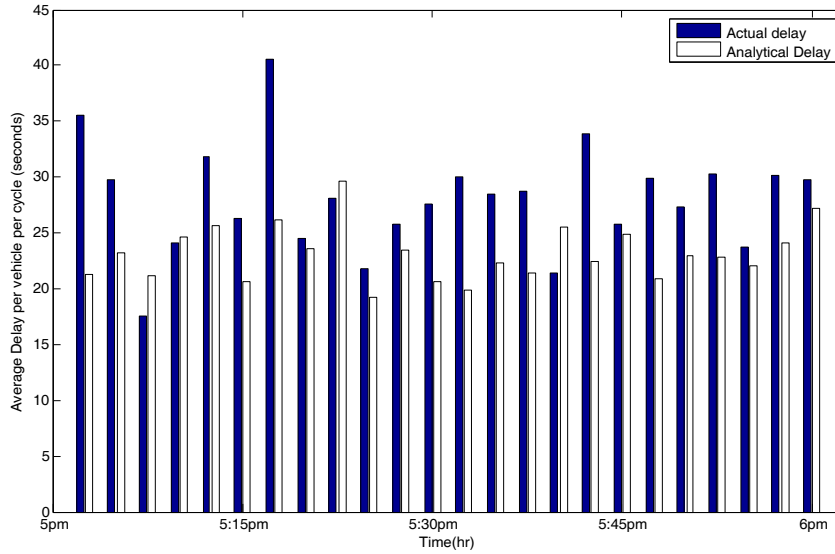
Figure 2.10 Measured vs. Calculated Delay for Through Movement--Leg 2
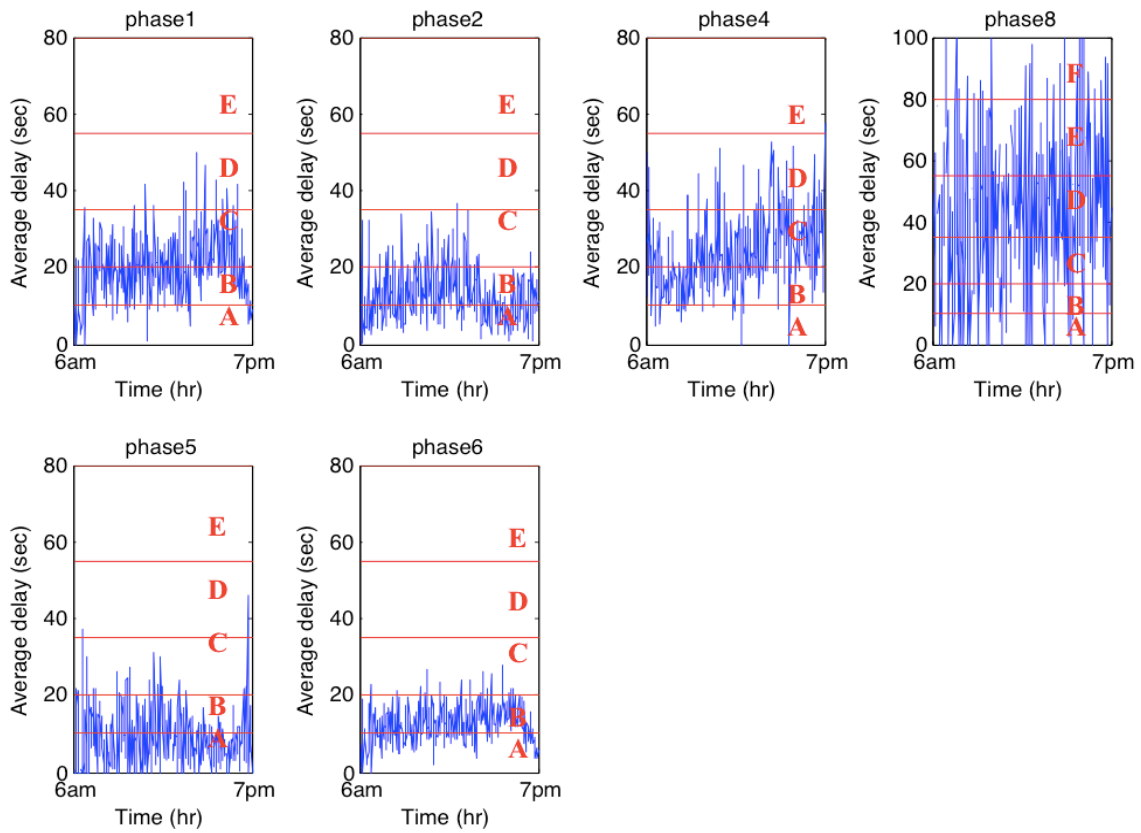
Figure 2.11 Average Delay per Phase with Level of service (LOS)

2.4.5 Queue length

The queue length per lane on each intersection approach is calculated from the HR data from vehicle arrivals at the upstream (advanced) and the downstream (stop-line) sensors. We developed a real-time estimation algorithm based on stochastic gradient descent that accounts for sensor measurement biases. Detailed description of the algorithm is described in a research paper attached as Appendix B. The general formulation is as follows:

$$\tilde{A}(t) - \tilde{D}(t) = A(t) - D(t) + \epsilon t \qquad (2\text{-}4)$$

Where:
$\tilde{A}$: the detected arrival counts over time t from the advanced sensor
$\tilde{D}$: the departure counts over time t from the stop-bar sensor
A,D: actual arrival and departure counts
ϵ the time dependent bias term

Figure 2.12 illustrates the difference between the actual and estimated queue length. Every busy period (time with a queue present) the algorithm updates the bias term value ϵ for the next busy period based on the previous bias term:

$$\hat{Q}(t) = \left[\hat{A}(t) - \hat{D}(t) - \epsilon_n * t\right]^+ \qquad (2\text{-}5)$$
$$\epsilon_{n+1} = \epsilon_n + \alpha_n * \Delta_n \qquad (2\text{-}6)$$

Where:
ϵ_{n+1}: the bias term for the next busy period, calculated from ϵ_n, the bias from previous busy period,
Δ_n: the difference between actual and estimated queue length at the end of the previous busy period
α_n: is the time step (predetermined value 3-5 sec)
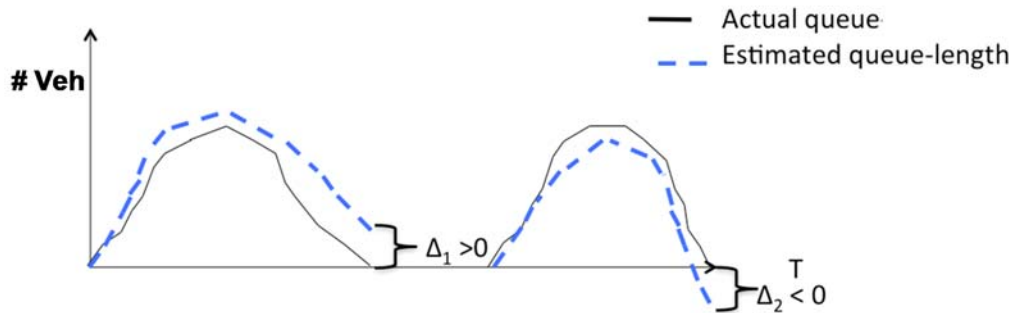
Figure 2.12 Queue Length Estimation

The algorithm was tested through simulation. Consider a single discrete-time queue that has Poisson arrivals with rate λ vehicles per 5 seconds time step. We set $\lambda = 1.4$ veh/ (5 sec) or 1,008 veh/hr. We consider a cycle time of 12 time steps (60 seconds) with 6 time steps of green and red time (30 seconds). The service time distribution is deterministic with service rate (saturation flow) $\mu = 0.6$ veh/sec = 2,160 veh/hr when the signal is green and $\mu = 0$ when the signal is red. Thus, the stability region of the queue is $\lambda < 1.5$.
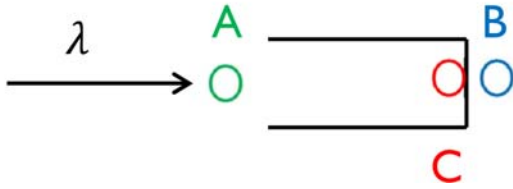
Figure 2.13 Detector's layout for Simulation

Figure 2.13 shows the assumed layout of three sensors for the "ideal" estimation of queue length. Sensor A counts the number of vehicles that enter the queue, sensor B counts the number of vehicles that exit the queue, and sensor C status indicates whether the queue is empty or not. We evaluate the performance of the proposed algorithm in two cases. First, we assume that sensor C is noiseless, sensor A counts each arriving vehicle with probability 0.95 independently, and sensor B counts each departing vehicle with probability 0.85 independently. Note that with the chosen parameters, we expect to see a bias $\varepsilon = (0.95 - 0.85) \lambda = 0.14$ vehicles per time slot. In the second case, we consider 2 modes of operation: (i) the first mode is the one explained before; (ii) the arrival rate is decreased to $\lambda = 1$ veh/ (5 sec) = 720 veh/hr. We assume that the system switches between these two modes every 2 hours or 1440 time slots. In this case, we choose a constant step size of $\alpha = 0.004$ so that the algorithm can adapt to the changes in the system. Note that the decaying step size enables us to prove the convergence of the correction term when ε is fixed. However, when $\varepsilon(t)$ is time-varying, the step size should be non-decaying so that learning does not stop. Recall that the step size is the learning rate of the algorithm. Thus, larger step size speeds up the learning. However, if the step size is chosen to be too large, the gradient-descent-based algorithm does not converge.

We now evaluate the performance of the proposed algorithm in the first case. We choose the step size $\alpha_n = 0.02/n^{0.6}$. Figure 2.14 shows how the correction term ε_n converges to the bias $\varepsilon = 0.14$. One observes that after only around 30 busy periods the algorithm learns the bias and gets close to 0.14. The estimated queue-length for a period of 5000 seconds is shown in Figure 2.15.
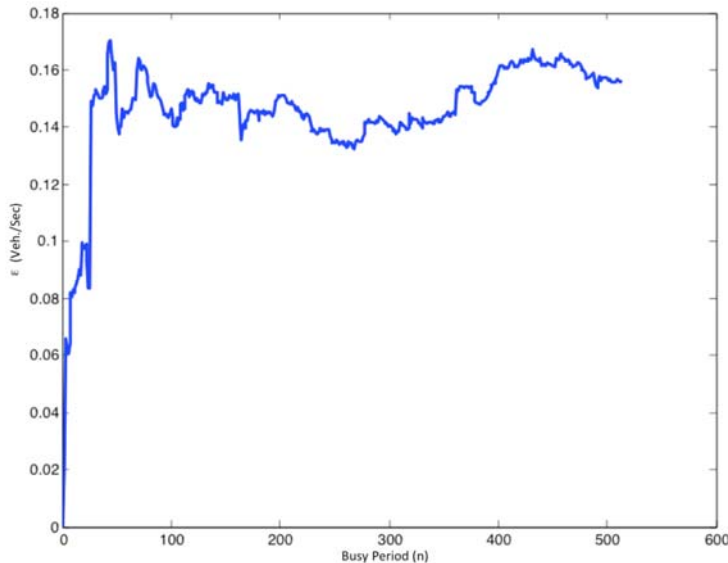
Figure 2.14 Error Convergence

At our real world test intersection, sensor C is not available to provide the exact time that queue is empty. We assume that if the signal is green by more than one time step (3 seconds) and no vehicle passes the stop-bar sensor then the queue is empty. Also, as soon as a vehicle passes the advanced sensor during the red interval, a queue starts to form. Figure 2.16 shows the estimated queue length for leg 1 through movement.
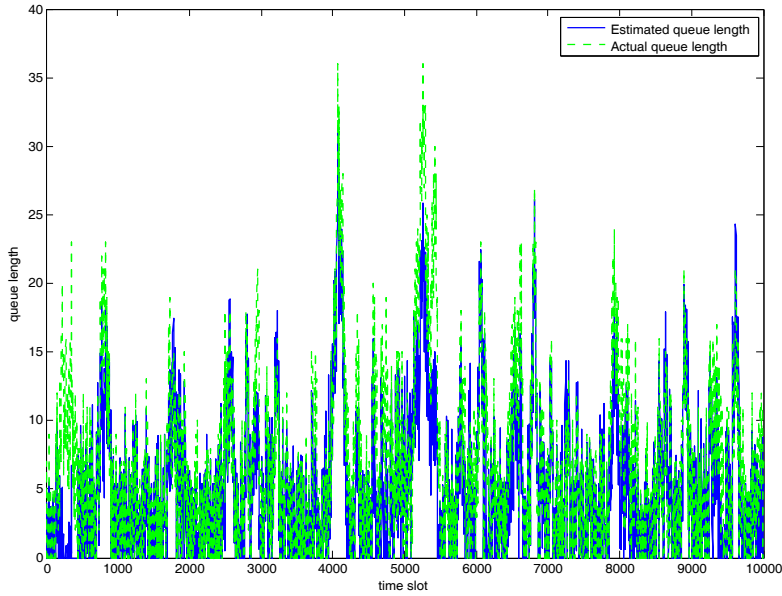
Figure 2.15 Actual vs. Estimated Queue Length
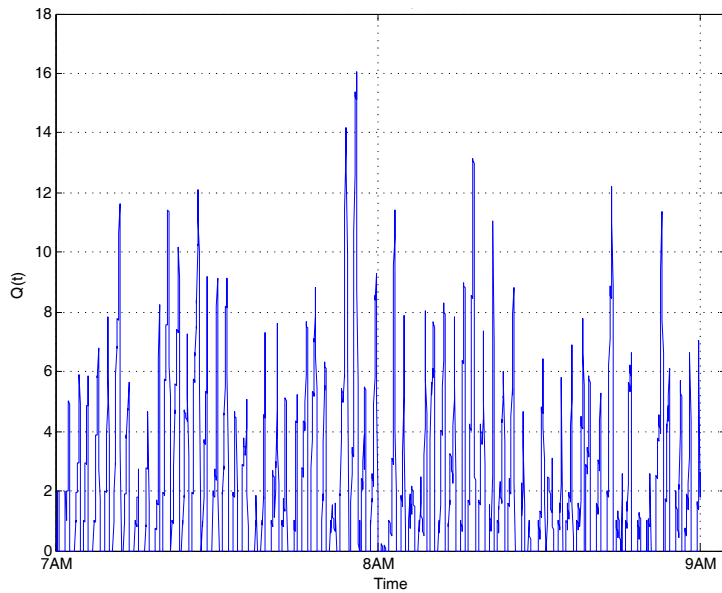
Figure 2.16 Queue Profile Leg 1 Through Movement

2.5 Application of HR data: Improving Signal Timing Plans

The typical approach for developing fixed time of day plans is to collect turning movement counts for certain times of the day (typically AM, midday and PM peak) and determine the signal settings (cycle length and green times) to minimize delay, stops or other chosen performance measures. These timing plans may not be optimal for other time periods or other days, because they don't account for the variability of traffic demand. Procedures have been proposed to develop robust timing plan to account for demand as well as supply variability but the high costs of collecting the required field data on turning movement counts makes most proposed approaches not practical [12]. The availability of continuous HR resolution data provides the opportunity to develop robust timing plans without additional costs.

Figure 2.17 shows the 5 min traffic volumes at the test intersection over the 12 hour analysis period. This information allows us to group (cluster) the data into periods of similar conditions to develop signal settings instead of predetermined time periods.
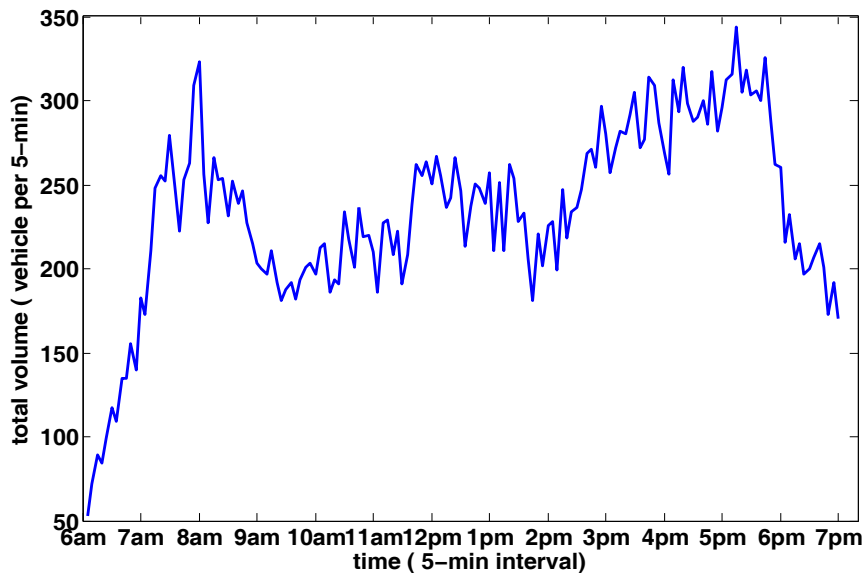
Figure 2.17 Total Volume at Test Intersection (#veh/5-min)

We used a K-means clustering method which partitions n observations (traffic volumes) in to k clusters in which observation belongs to the cluster with nearest mean. The objective is to minimize the distance of every item in each cluster from the center of the cluster, as it is shown in the following equation:

$$\underset{S}{\operatorname{argmin}} \sum_{i=1}^{k} \sum_{x \in S_i} \| x - \mu_i \| \qquad (2\text{-}7)$$

Where, x presents each point from group S_i.

In our case we have K=3 clusters because we have three timing plans. The process consist of the following steps: a) estimate the center of each group, b) calculate the distance of each point from the center points, c) put each point in the group with the least distance from the center, d) go back to step (b) and continue this process until no point leaves its group in step (c). Figure 2.18 shows the points in each cluster obtained from the application of the method.

16
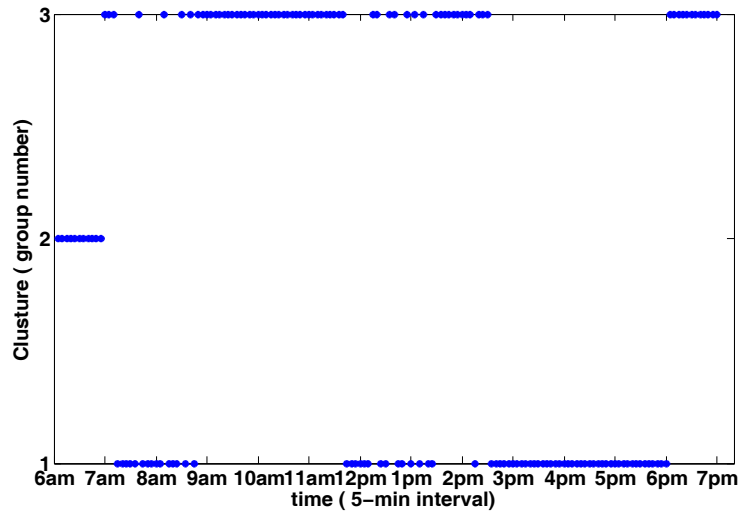
Figure 2.18 Clustering of Volume Data, February 18, 2015

We developed three signal timing plans using the clustered volumes, using the SYNCHRO widely used signal optimization software [11]. Figure 2.19 shows a comparison of existing and new timing plans. It can be seen that the proposed timing plans improved the intersection delay by 10% on the average over the existing signal timing plans. As it was expected the higher benefits obtained over the time periods of beginning or dissipation of designated peak periods (e.g., 9 AM and 4 PM).
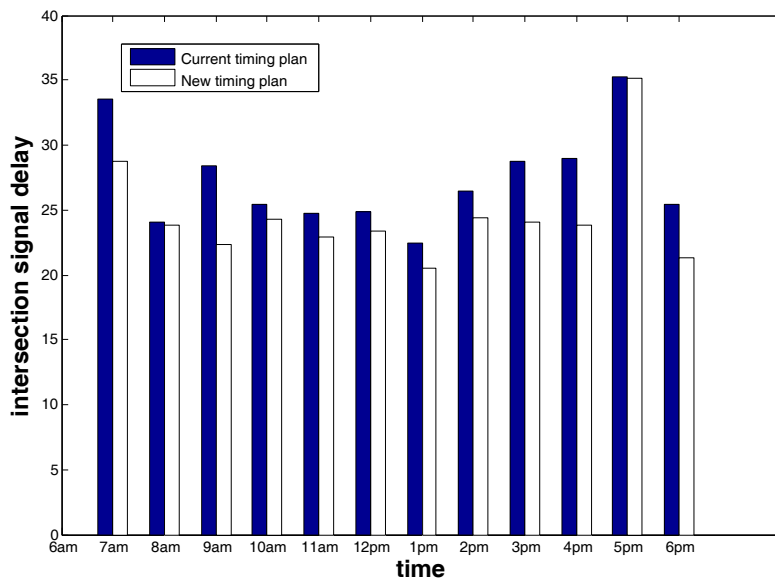
Figure 2.19 Existing vs. Proposed Timing Plans

CHAPTER 3

THE PointQ SIMULATION MODEL

This Chapter describes the application and findings of the PointQ model under development at UC Berkeley [13] on real-world study sites.

3.1 PointQ model Description

PointQ is a microscopic (vehicle-by-vehicle) simulator which models a network of signalized intersections as a network of controlled queues, with one queue per movement or phase, similar to a store-and-forward communication network. Vehicles enter the network at the entry links according to a deterministic or random (poison) process. They travel along a link in a fixed or random travel time. At the end of the link they join a queue. Vehicles make turns at intersections either in fixed proportions or according to a randomly selected origin-destination (O-D) route and leave the network when reach an exit link.

PointQ combines the advantages of microsimulation, it tracks individual vehicles, so it can model O-D demands and calculate individual vehicle travel times and delay, with those of macrosimulation, i.e., it does not model individual car-following/lane changing dynamics. The model has been validated based on the detailed trajectory data from the FHWA's Next Generation Simulation (NGSIM) database [14]. It can be interconnected with macroscopic freeway simulators to model integrated freeway-arterial traffic networks. Also, it has been interfaced with the Maximum Pressure signal control algorithm to determine signal settings [15].

PointQ is a discrete event simulator. Events are related to the system entities: vehicles, traffic controls, and the physical network (comprised of signalized and non-signalized intersection nodes, their corresponding input and output links and the vehicle queues modeled according to the related phases to each link). The occurrence of an event modifies the system state according to the related procedure and may also create new events of any type and nature. In Figure 3.1 the nodes shown represent the different event types and edges indicate the generation of an event. The following events are generated in the simulation:

> Type 1: appearance of a new vehicle in a signalized network node
> Type 2: decision for the next intersection control
> Type 3: a new stage is applied to the intersection
> Type 4: vehicle leaves a signalized queue
> Type 5: vehicle arrives at a signalized queue
> Type 6: vehicle achieves its hold constraint imposed by a store and forward model (case of a signalized intersection)
> Type 7: flow variations
> Type 8: vehicle appears at a non-signalized intersection
> Type 9: vehicle ceases its store and forward hold time in a non-signalized queue
> Type 10: vehicle departs from a non-signalized intersection.
> Type 11: vehicle joins a non-signalized intersection queue

The vehicle departure events concern one or more vehicles according to the number of the vehicles which can leave the queue simultaneously. This number depends upon the input saturation flow rate.

Events of types 6, 11 correspond to a store and forward model, and impose a minimum hold time in the queue. Events related to non-signalized intersections need to be updated to the current version of the PointQ handling control requiring sensor information.

1: veh appear sign node
2: decision new inters ctrl
3: new inters ctrl
4: veh departs
5: veh arrival
6: end veh hold at que
7: flow variation
8: veh appear non-sign node
9: end veh hold non-sign node
10: veh departs non-sign node
11: veh arrival non-sign node
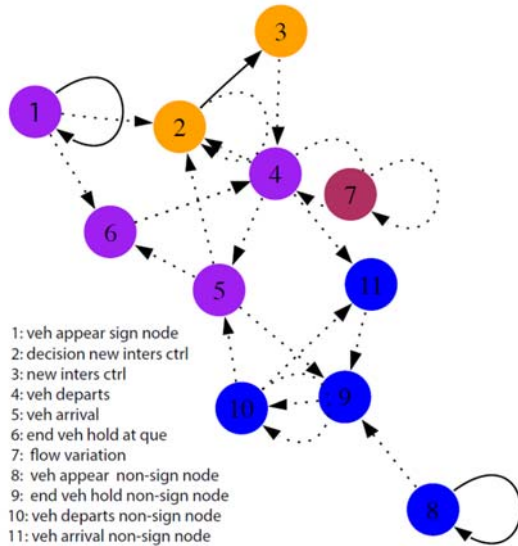
Figure 3.1 Sequence of the PointQ Model Events

The PointQ model requires the following input data:

1. Network characteristics: allowable movements, saturation flow for each movement (i.e., number of lanes), link storage capacity (number of vehicles, including turn pockets), link travel time (i.e., speed, constant or stochastic). Because the model does not explicitly consider the lane configuration at the intersection approaches, only saturation flows per movement, the saturation flows for shared lanes (e.g., through and right turn movements) are input proportional to the movement volumes.

2. Traffic demand: flows at each entry link, turn ratios for each movement at every intersection and/or origin-destination (O-D) flows.

3. Signal timing data: Specification of timing plan at each intersection (phase green times, cycle length, and offsets).

The output of PointQ model consists of a record of all the events in the simulation run, including both vehicle events and intersection traffic control events. The processing of the model output by the model user, produces several network performance measures including link and route travel times, vehicle-miles traveled (VMT), and intersection/link performance measures (queues, delays). For example, the simulation output lists for each vehicle the time when it joined the queue and the time when it left the queue. The difference provides the time that each vehicle spent in the queue.

3.2 Application on Real-World Test Sites

3.2.1 Isolated Intersection: Ribaut Rd @ Lady's Island Drive, Beaufort, SC

The pointQ model was applied to evaluate the performance of the Ribaut Rd/Lady's Island Drive intersection in Beaufort, SC, which was used in the collection and analysis of HR data, described in Chapter 2. Figure 3.2 shows the layout of the intersection and the link designation for the pointQ model. Also shown are the green times per phase with a fixed cycle length of 110 seconds. We simulated two hours of operation (6 to 8 am) when conflicting legs 2 and 3 have the highest traffic demand. Saturation flow rates were set as 1,800 vphg/lane.
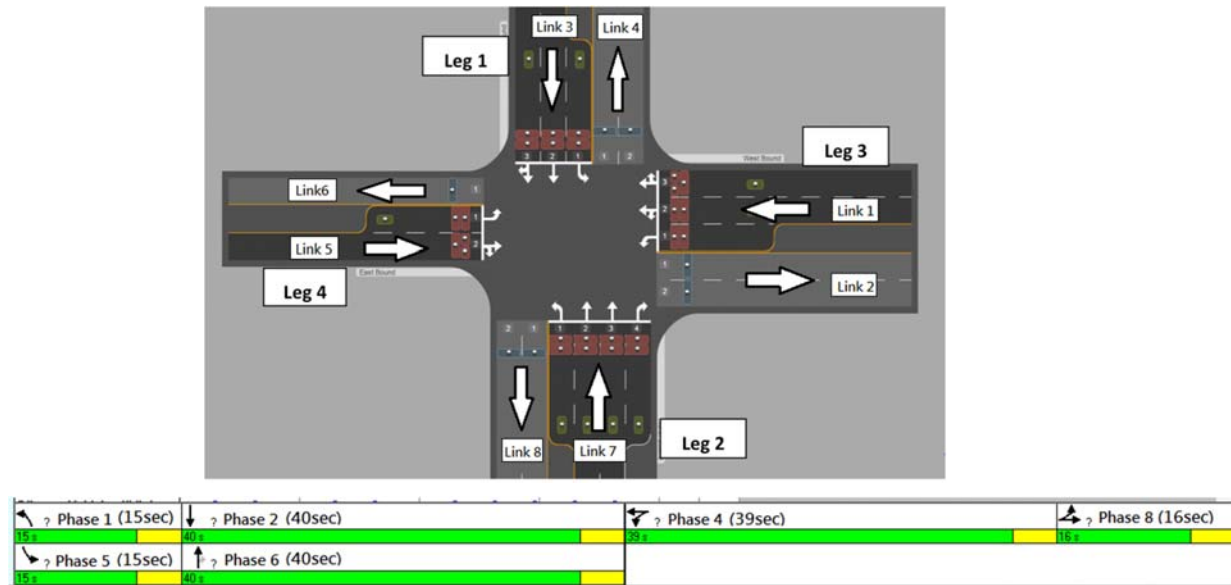
Figure 3.2 Test Intersection Layout and Signal Settings

The data output for the queue length from the pointQ model is in the form of a graph of queue length in number of vehicles vs. time of simulation (Figure 3.3). The average queue is calculated from the total output area below the blue line shown in Figure 3.3 and divided by the entire time period (In this case is 1 hour, 6-7 AM). The maximum queue length is the highest point in the graph.
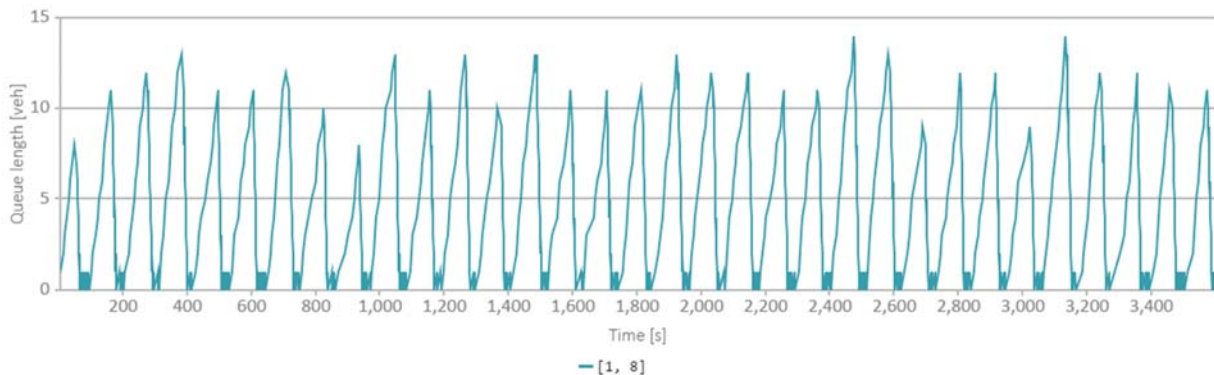
Figure 3.3 PointQ Predicted Queue Link1 to Link 8

20

We also modeled the test arterial using the widely used SYNCHRO traffic analysis and optimization software [11], and compared the SYNCHRO measures against the pointQ predictions. Table 3.1 shows the estimated maximum queue lengths from the two models.

The SYNCHRO model calcuates queue lengths based on the HCM procedures as shown in Figure 3.4. A single signal cycle is modeled and the average end of queue (in ft) is computed from the input flows, saturation flows and signal settings. Also SYNCHRO does not report the maximum queue length; it reports the 95th queue length, which is calculated as twice the average queue length. Because the predicted queue length from PointQ is in number of vehicles, we assumed an average vehicle length is 25 feet to convert the queue estimates in feet by SYNCHRO into number of vehicles to compare with pointQ.
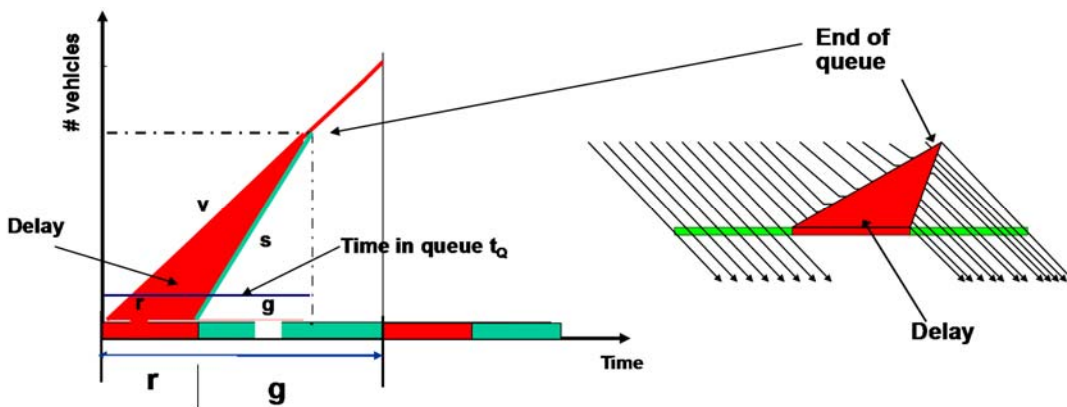
Figure 3.4 SYNCHRO Queue Length Estimation

Table 3.1 shows that the predicted maximum queues from the two models are in reasonably close agreement, given the differences of estimating the queue lengths among the two models. The differences are within one or two vehicles for most of the intersection movements. Significant differences are found on through and right turn movements on Leg 2. In this leg, the right turn movement has an exclusive lane that allows traffic to move during the red time during non cnflicting phases. However, right turn on red and overlaps are not modeled in pointQ.

Table 3.1 Maximum Queue Lengths: PointQ vs. SYNCHRO (# veh)

MODEL/	LEG 1 (SB)		LEG 2 (NB)			LEG 3 (WB)		LEG 4 (EB)	
TIME PERIOD	LT	THR	LT	TH	RT	LT	THR	LT	THR
6:00-7:00 AM									
.Q	12	7	2	11	9	18	7	3	3
SYNCHRO	15	6	2	6	3	14	9	2	4
7:00-8:00 AM									
.Q	7	7	2	14	10	14	6	2	2
SYNCHRO	7	7	2	8	3	12	8	2	2

3.2.2 Arterial: San Pablo Avenue, Berkeley, CA

The PointQ model was applied to assess the traffic performance of a section of San Pablo arterial in the city of Berkeley, California. The study section includes ten signalized intersections along San Pablo Avenue, from Ashby Avenue to Gilman Street (Figure 3.5). The distance between intersections ranges from 450 to 1983 ft, for a total length of 2.02 miles. The posted speed limit is 35 mph. Traffic demand data consist of turning movement counts for the PM peak hour (4-5 pm). All signals operate as fixed-time coordinated with a common cycle length of 80 seconds.

Figure 3.6 shows the link-node numbering scheme for the PointQ model application. There are a total of 10 nodes and 52 links.
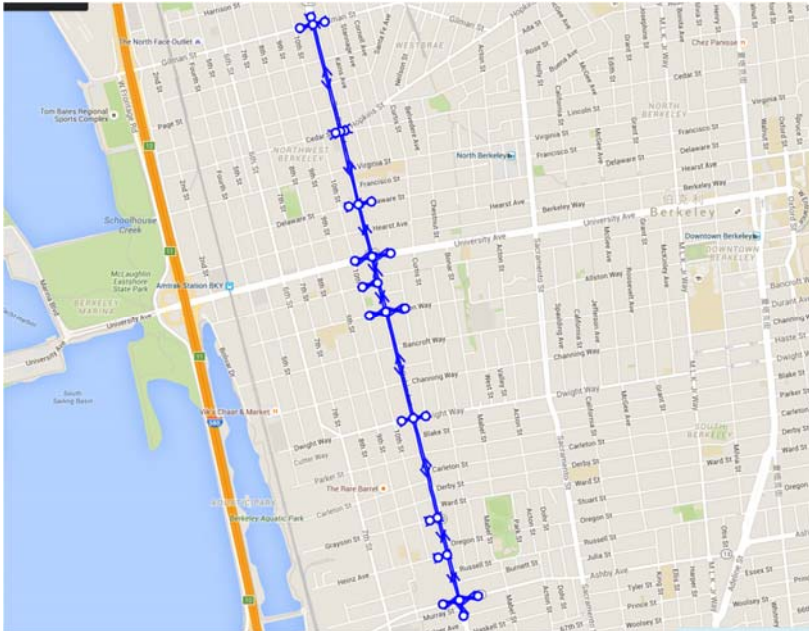
Figure 3.5 Map of San Pablo Test Arterial
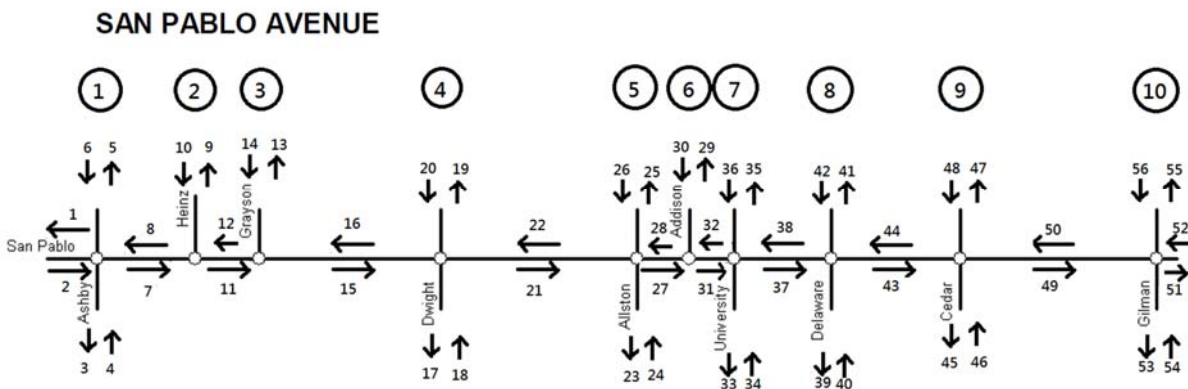
Figure 3.6 PointQ Model Link & Node ID for Test Arterial

We performed a one hour simulation with the PointQ model and processed the output to obtain performance measures namely travel times on the arterial, and queue lengths at intersection approaches of critical intersections. We also modeled the test arterial using the SYNCHRO software, and compared the SYNCHRO predicted performance measures against the pointQ

22

predictions. We performed two series of simulation experiments: a) existing signal settings, and b) SYNCHRO optimized signal settings (green times and offsets). The findings are presented below:

Arterial Travel Time:

Table 3.2 shows the average travel times along the arterial per travel direction for each signal control scenario. The predicted travel times are in close agreement especially under the optimized signal settings. There is a 16% difference in travel times between SYNCHRO and pointQ in the NB direction of the arterial under the existing signal settings. To better understand the travel time predictions we compared the link travel times on each segment (link) as shown in Figure 3.7. It can be seen that the link travel times are very close except on Link 15 (northbound approach on San Pablo and Dwight Way) which also explains the 16% difference on the arterial travel time (Table 3.2). This is because SYNCHRO over-predicts the delays at intersection approaches such as northbound Dwight Way that is close to saturation. This results in long travel times for the particular link.

Table 3.2 Arterial Travel Times: PointQ vs. SYNCHRO (minutes)

ARTERIAL DIRECTION	EXISTING SIGNAL TIMINGS			OPTIMIZED SIGNAL TIMINGS		
	.Q	SYNCHRO	DIFF	.Q	SYNCHRO	DIFF
Northbound	4.95	5.90	16.10%	4.53	4.57	0.73%
Southbound	4.23	4.63	8.63%	4.55	4.73	3.87%
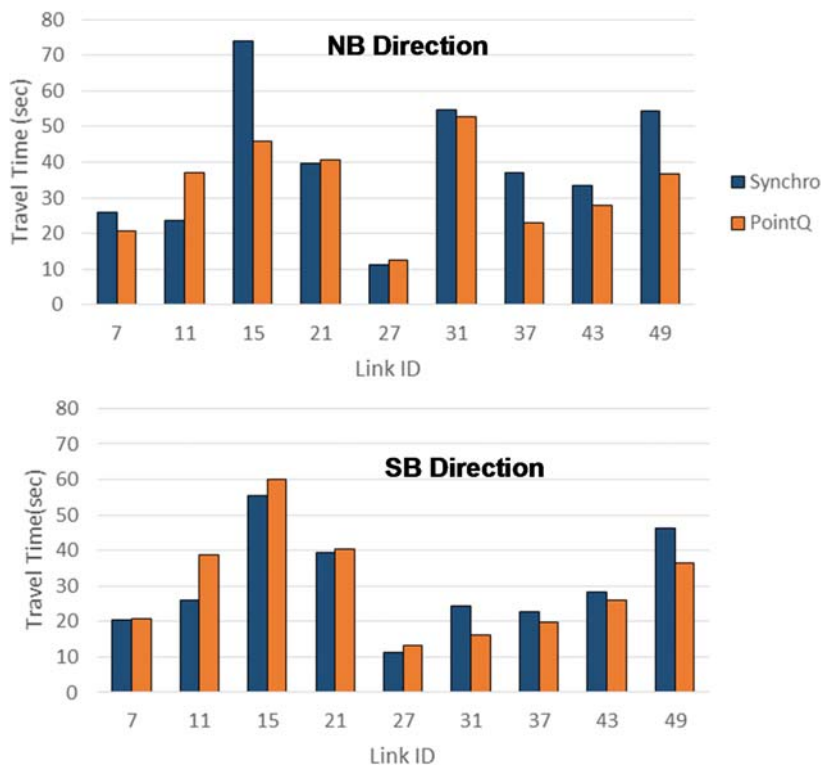
Figure 3.7 Link Travel Times – Existing Signal Settings

Figure 3.8 shows the travel time by link for two models after the optimization of signal settings. The travel times from the two models are very close at all links. The signal optimization provided additional green time on link 15 which eliminated the oversaturation and high delays predicted by the SYNCHRO model in the case of existing signal settings (Figure 3.7).
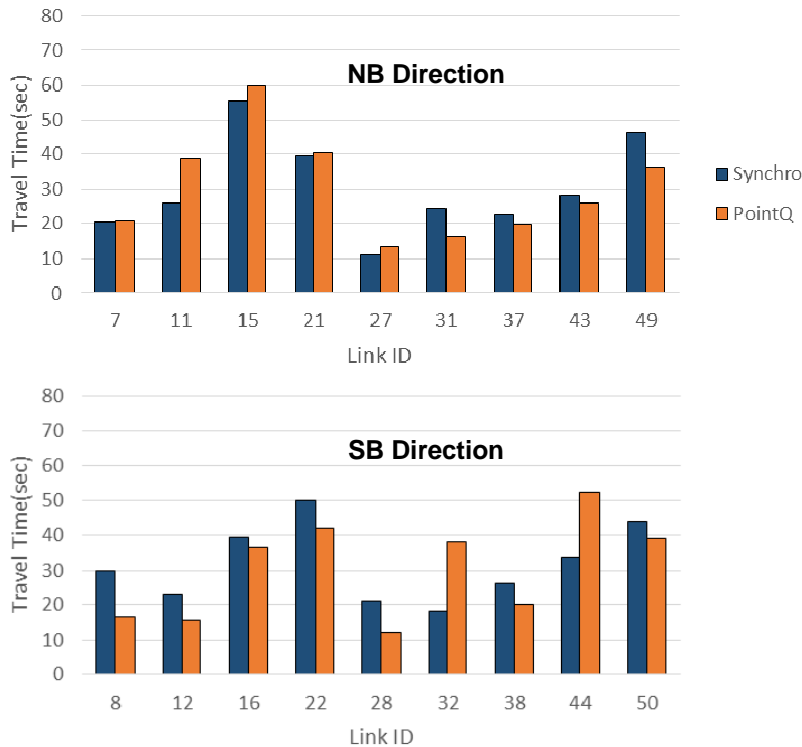
Figure 3.8 Link Travel Times – Optimized Signal Settings

Queue Length:

Figure 3.9 shows a comparison of maximum queue lengths under optimized signal control for three intersections on the arterial: San Pablo & Dwight, San Pablo & University and San Pablo & Gilman. The queue lengths are similar except on the San Pablo & Dwight and San Pablo & Gilman intersections where there are shared lanes (through and right turns) with significant right turning traffic.
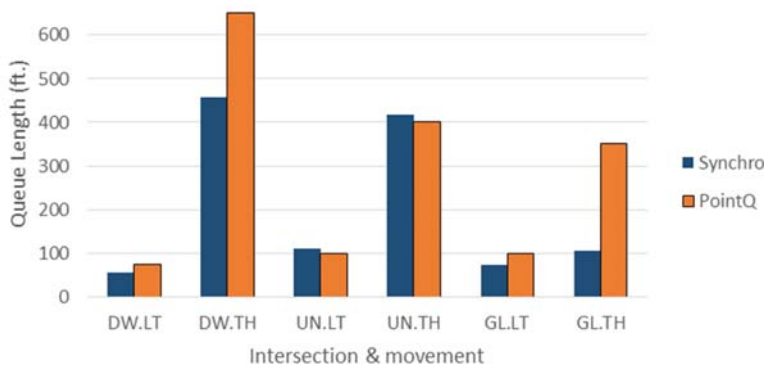
Figure 3.9 Maximum Queue Length

CHAPTER 4

FREEWAY-ARTERIAL COORDINATION STRATEGIES

Several efforts are underway for integrated corridor management (ICM) of facilities comprised of freeways and adjacent arterial streets [16]. One of the main obstacles toward an efficient management of a travel corridor is the coordination of the various subsystems that it comprises. The divisions between these subsystems are drawn along jurisdictional boundaries which often have little to do with travel patterns.

A guide published by FHWA [17] describes the challenges for arterial–freeway coordination and suggests procedures to facilitate integration. The document focuses mainly on planning, institutional issues and data dissemination, and less on the development of control strategies that can be implemented in real time. Existing research has focused on development of optimization algorithms and routing models for integrated control of freeway-arterial corridor system [18,19,20,21] with emphasis on non recurring congestion. Other approaches focus on control strategies for freeway interchanges [22,23,24]. In this research we focus on a) control strategies that prevent overflow on metered ramps that adversely affect arterial operations under recurrent congestion, and b) guidance on traffic diversion from freeway to arterials in the case of non recurrent (incident related) congestion.

4.1 Recurrent Congestion—Queue Overflow at Metered Freeway On-Ramps

The objective of freeway on-ramp metering is to regulate the entry of vehicles to prevent congestion on the freeway mainline. Several ramp metering algorithms have been developed and implemented worldwide [25]. Most of the operational ramp metering systems employ a "queue override" feature that is intended to prevent the on-ramp queue from obstructing traffic conditions along the adjacent surface streets. The override is triggered whenever a sensor placed at the entrance of the on-ramp detects a waiting queue of the on-ramp vehicles, and increases the metering rate to its maximum value, to empty the queue into the freeway.

The queue override reduces the effectiveness of employed ramp metering systems during the time of highest traffic demand, when the ramp metering is most needed. Significant benefits can be realized by preventing the queue override. This can be accomplished by i) developing ramp metering strategies that take into account the on-ramp queues, ii) managing the on-ramp demands from the adjacent surface street with signal control strategies.

Earlier research at the PATH program developed an on-line ramp metering strategy that considered the on-ramp queue lengths in the determination of ramp metering rates [26]. Figure 4.1 illustrates the approach. The top of Figure 4.1 shows that under the conventional ramp metering algorithm the queue exceeds the on-ramp queue threshold shown by the red line, triggering queue override. The bottom of 4.1 shows the queues under the new ramp metering strategy. The algorithm keeps the ramp queues under the threshold avoiding the queue override.
This strategy requires the measurement of the on-ramp queue which is difficult in practice.
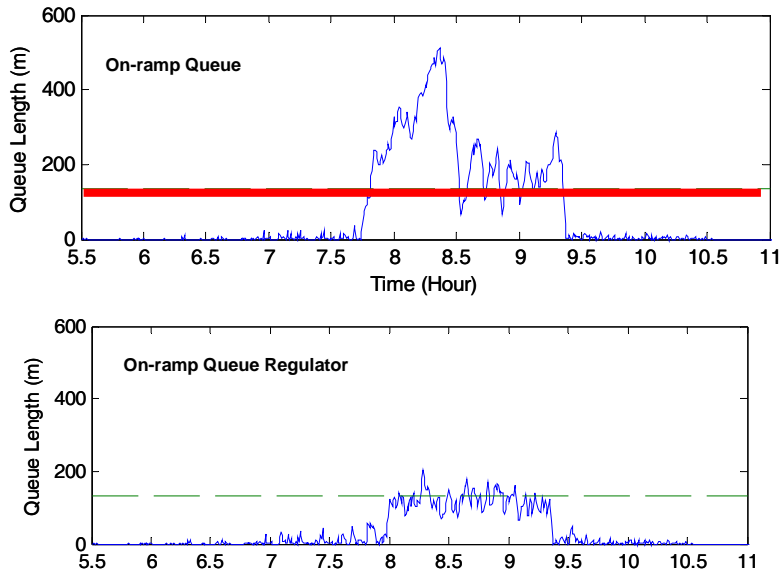
Figure 4.1 Queue Regulator Ramp Metering Strategy [25]

In this research project we developed a control algorithm to manage the entry of vehicles on the on-ramp through signal control changes at the adjacent intersection(s). The algorithm is an extension of a control algorithm that was originally developed for coordination of a single freeway metered on-ramp with an adjacent isolated signalized intersection [8]. The algorithm considers several signalized intersections along the parallel arterial and assumes that the metering rates and algorithms are fixed, i.e., the focus is on the adjustment of signal settings at the neighboring signals.

The proposed strategy adjusts the green times and offsets on the arterial traffic signals with the objective that on-ramp queues do not exceed the on-ramp queue storage (Figure 4.2). The following objectives must be satisfied: i) minimum green times at each signal phase, ii) fixed cycle time, and iii) available storage on the arterial links as shown in Figure 4.2.
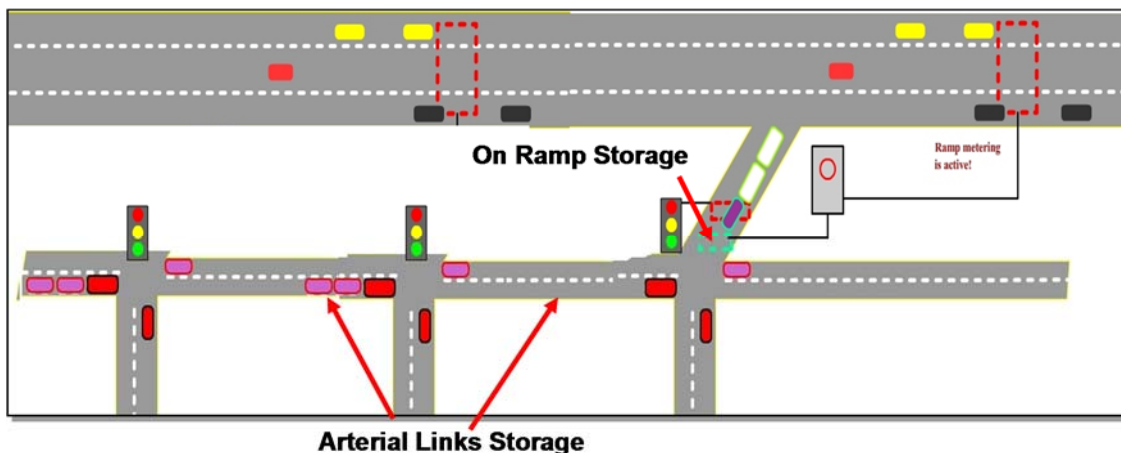
Figure 4.2 Freeway-Arterial Control Strategy

We tested the proposed strategy on a real-world freeway segment and parallel arterial. The test site is a 4 mile section of I-680 in the northbound direction, and a parallel arterial Capitol Avenue with three signalized intersections in the city of San Jose, California (Figure 4.3). The selected freeway section has four lanes in each direction, whereas the parallel arterial Capitol Ave., as well as Alum Rock Ave. and Berryessa Rd. all have two lanes in each direction. McKee Rd. has three lanes in each direction. The on-ramp meters operate under the local responsive demand-capacity strategy, and the arterial traffic signals operate with time of day (TOD) coordinated actuated timing plans.

There are three recurrent bottlenecks in this freeway section, located near the on-ramps from Berryessa Rd., McKee Rd., and Alum Rock Ave. These bottlenecks are caused by the high on-ramp merging traffic entering the freeway mainline from of the westbound direction of Berryessa Rd., McKee Rd., or Alum Rock Ave., along with high on-ramp demand from both directions of Capitol Ave., during the morning peak period (7:30-9:30 AM). Figure 4.4 is a contour plot of average speeds of the selected freeway segment during a typical morning peak period. Figure 4.5 shows the flow and speed at the bottleneck near Alum Rock Avenue.
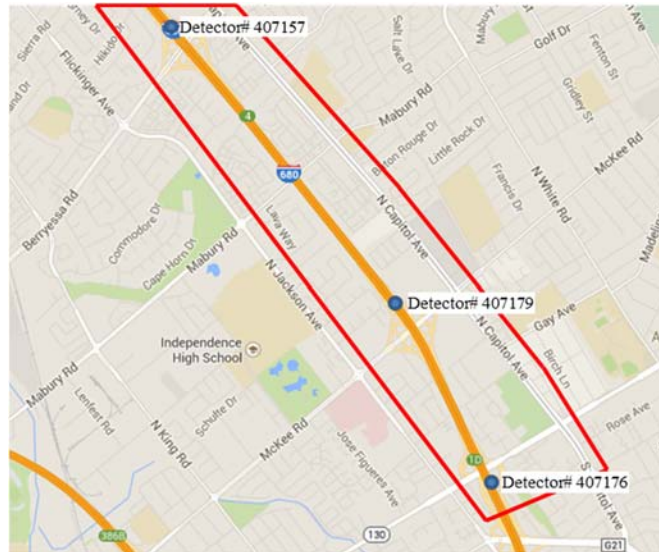
Figure 4.3 Study site: I-680-Capitol Ave and Detector Locations

The selected site was coded into the AIMSUN [27] microscopic simulation model. Freeway input demands and performance data were obtained from the PeMS system [28], which stores detector data (flow, speed, occupancy) aggregated over 5 minutes. For the arterial intersections, 5-minute turning moment traffic counts were collected. Ramp metering rates and signal timing plans were obtained from Caltrans and the city of San Jose.

The model was calibrated to existing traffic conditions by adjusting input data and model parameters. The predicted flows and speeds at selected locations on the freeway mainline were compared with real traffic measurements in every 5 minutes to assess the accuracy of the simulation model in representing observed conditions. The GEH criterion was used to assess the

agreement of simulated predictions and field measured flows [28]. According to this criterion, simulated flow quantity is said to be acceptable if it satisfies the following requirements.

Link flow quantity
- If 700vph < real flow < 2700vph, simulated flow has an error within 15%;
- If real flow < 700vph, simulated flow has an error within 100vph;
- If real flow > 2700vph, simulated flow has an error within 400vph.

The GEH statistic is computed as:

$$GEH(k) = \sqrt{\frac{2[M(k) - C(k)]^2}{M(k) + C(k)}} \qquad (4\text{-}1)$$

where:

$M(k)$ is the simulated flow in time interval k.

$C(k)$ is the corresponding field measured flow in time interval k.
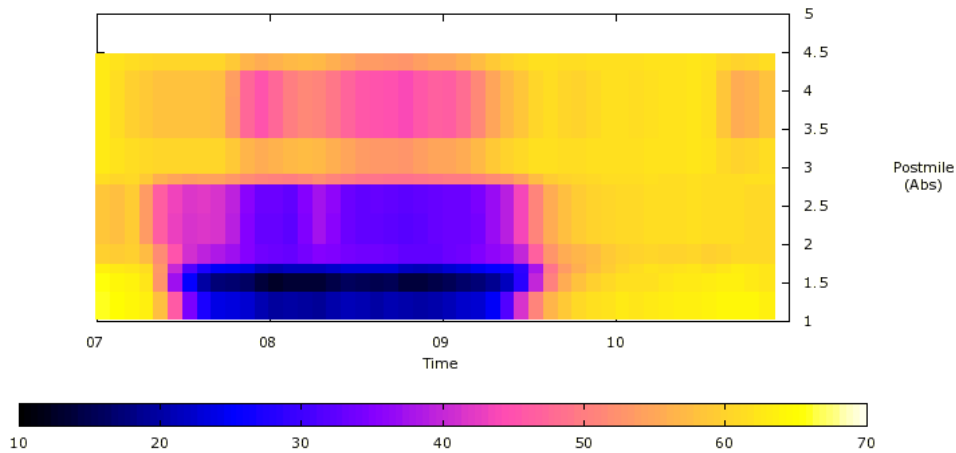
Figure 4.4 Speed Contour plot of NB I-680 Test Section
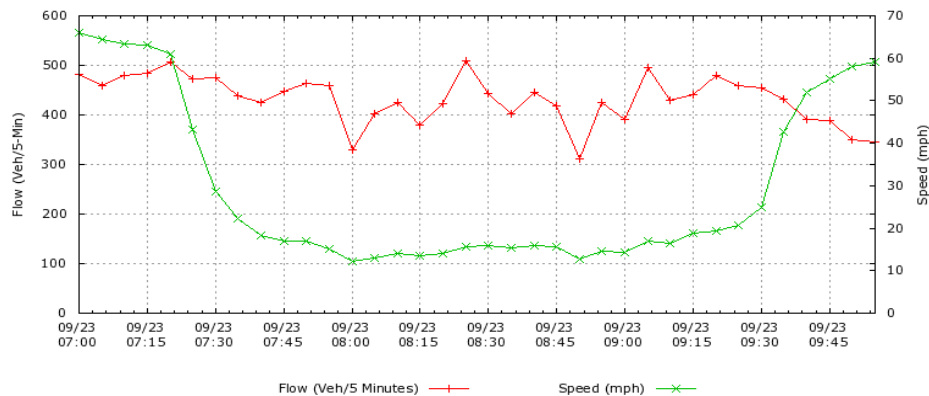
Figure 4.5 NB I-680 Flow and speed at Alum Rock Ave. on-ramp

A satisfactory calibration requires that the predicted freeway flow satisfies the condition GEH < 5 for at least 85% of all 5-minute time intervals. For speed, the relative root mean squared error (RRMSE) of the simulated speed values is required to be 15% or lower, on average of all detectors. For arterial flows, the GEH < 5 criterion must be satisfied for at least 85% of all 5-minute time intervals, for each turning movement of the major intersections. The results from the model calibration show that he model satisfies the simulation acceptance criteria. On the arterial links, the above mentioned flow criteria were satisfied 95% of the time. Figure 4.6 shows that the field measured and simulated freeway speeds are in close agreement.
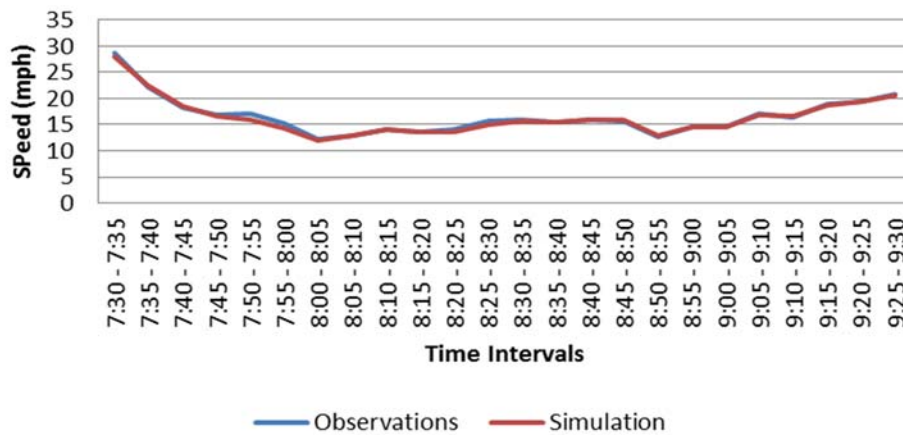
Figure 4.6 Observed vs. simulated speeds on NB I-680 at Alum Rock Ave. on-Ramp

The proposed freeway-arterial coordination strategy was tested using the calibrated simulation model. The results were analyzed separately for a) freeway traffic, b) arterial through traffic, c) arterial on-ramp traffic, and d) total system. The results are shown in Figure 4.7 in terms of percent improvements in delay due to the proposed strategy compared to the existing operations.

The proposed coordination strategy improved the performance of the freeway as expected. The delay was reduced by 15%, and the throughput was increased by 3%. Figure 4.8 shows the proposed strategy improves the bottleneck discharge flow.

On the arterial the strategy produced mixed results. The delay was reduced on travel directions/movements that do not intend to access the freeway on-ramp on both Capitol Ave. and McKee Rd arterials, and the delay increased on the approaches serving the on-ramp traffic. This is because these movements received additional green time when the green times on the phases serving the on-ramp traffic were reduced to prevent the queue overflow on the on-ramp. However, the delay increase did not create operational issues on those links. On the average, the delay on arterial through traffic was reduced by 15%, and the delay for the on-ramp serving traffic originating from northbound Capitol Ave. and westbound McKee Rd was increased by 5%.
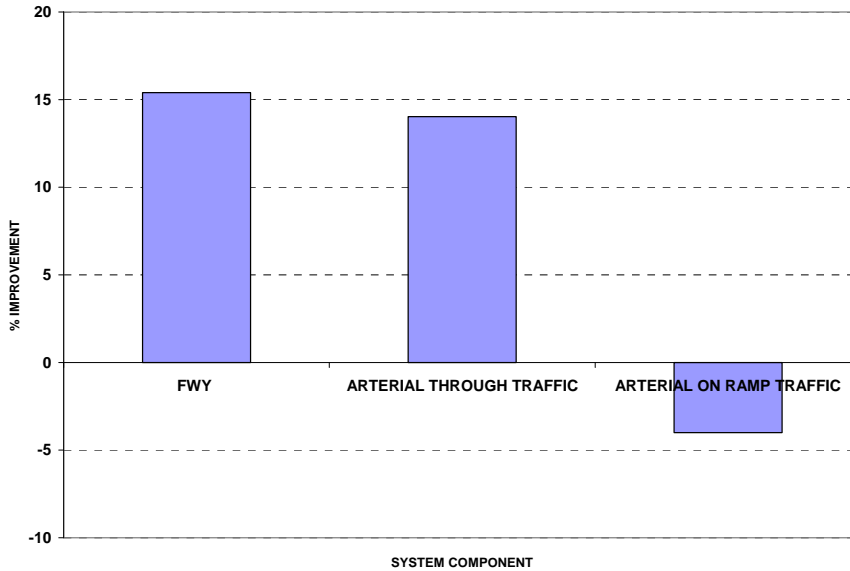
Figure 4.7 Delay Impacts of Freeway-Arterial Coordination Strategy
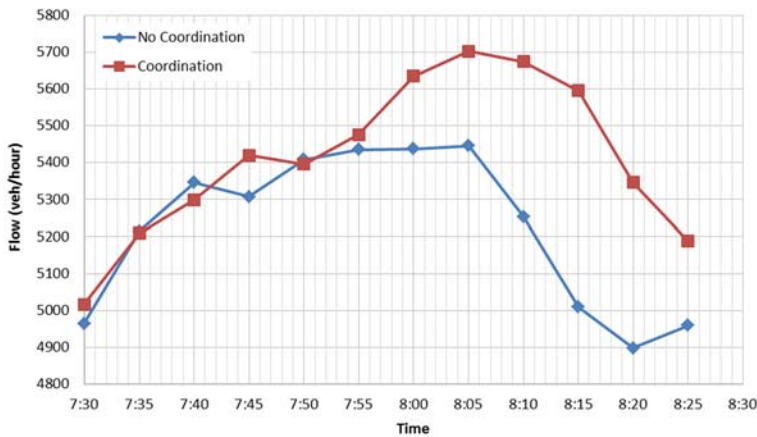
Figure 4.8 Impacts of Freeway-Arterial Coordination: Freeway Bottleneck Flow

4.2 Non-Recurrent Congestion –Incident on Freeway

A commonly recommended strategy for freeway/arterial coordination in ICM projects [16] is the use of parallel arterial(s) as reliever route(s) to the freeway travelers whenever there is a capacity reducing incident on the freeway. In this situation, drivers may be instructed to divert on the parallel arterial(s) and return to the freeway past the incident location. The signal settings on the arterial are set to facilitate the movement of the diverted freeway travelers ("flush plans"). As we discussed several models have been developed to provide alternative routes and estimate the benefits of diversion [20,21]. However, there is no empirical evidence yet on the effectiveness of such strategies, and there is no clear understanding of the issues involved in the development and implementation of these strategies. The Freeway-Arterial coordination handbook [17] provides mostly information on interagency coordination but not technical guidance on estimating allowable diversion volumes and associated impact.

30

The effectiveness of diversion strategies largely depends on accurate prediction of the diverted volume on the parallel arterial and deployment of signal settings on the arterial to accommodate the diverted traffic. Critical considerations for diversion strategies include but are not limited to:

- Freeway operating conditions: level of congestion, bottleneck presence and causes and impacts, origin-destination patterns

- Incident location, severity and duration: lane-blocking incidents located at or close to existing recurrent bottlenecks create significantly higher adverse impacts as opposed to short duration incidents upstream of bottlenecks

- Characteristics of the traveler information system: Drivers consider diversion to parallel arterials based on travel information (e.g., changeable message signs, in-vehicle information systems), and their compliance rate depends on the characteristics of travel information (type, accuracy and timelines) and the perceived congestion level.

- Surveillance and control system in place: location and type of sensors along the freeway and the parallel arterial(s) that provide real-time data, ramp metering and arterial control system features

- Characteristics of the parallel arterial: Amount of the spare capacity at the critical intersection along the parallel arterial. Trade-offs between the delay on the background arterial traffic with the existing settings and the capacity maximizing settings to facilitate the freeway diverted traffic.

The amount of diverted traffic to the parallel arterial depends on the available capacity at the critical intersection along the arterial. It can be estimated as follows:

$$dVi = \frac{RCi}{Xi} 100 \qquad\qquad (4\text{-}2)$$

Where:
dV_i : additional traffic volume on approach i *(%)*
X_i : degree of saturation (volume/capacity) on approach i *(%)*
RC_i : reserve capacity on approach $i = 1\text{-} X_i$

The formula (4-2) assumes that the critical intersection (and arterial) operate under capacity maximization settings, i.e., the cycle length and green times are optimize to maximize the reserve capacity at the critical intersection approaches. Figure 4.9 shows the amount of additional volume in (%) as a function of the volume/capacity ratio at the critical intersection approach. For example, assuming a two lane through movement at a traffic signal operating under 80% degree of saturation and green ratio of 50% it can accommodate 360 diverted vehicles.

The diverted volume can be thought as a gain in the reduced capacity of the freeway due to the incident, i.e., less reduction in remaining freeway capacity. Figure 4.10 shows the estimated loss of freeway capacity in the case of an incident blocking one lane. In the case of no diversion or no available capacity on the arterial, the capacity loss ranges from 42 to 29% depending on the number of freeway lanes [10]. Traffic diversion on the arterial facilities is equivalent of capacity gain on the freeway, i.e., the incident related capacity loss is reduced. As shown in Figure 4.8 if the

available spare capacity at the critical intersection is 0.40, there is essentially no capacity loss due to the incident.

The above estimates are based on several assumptions related to the traffic characteristics and operations. It is assumed that all drivers will divert and the signal operations will operate at capacity. At the same time they provide a planning level methodology on the potential of diversion at selected corridors given the characteristics of parallel arterials before investing in detailed simulation analyses and implementation scenarios. The approach can be extended and generalized to cover different incident characteristics (multilane blockages), freeway characteristics and arterial system (e.g., multiple alternate routes).
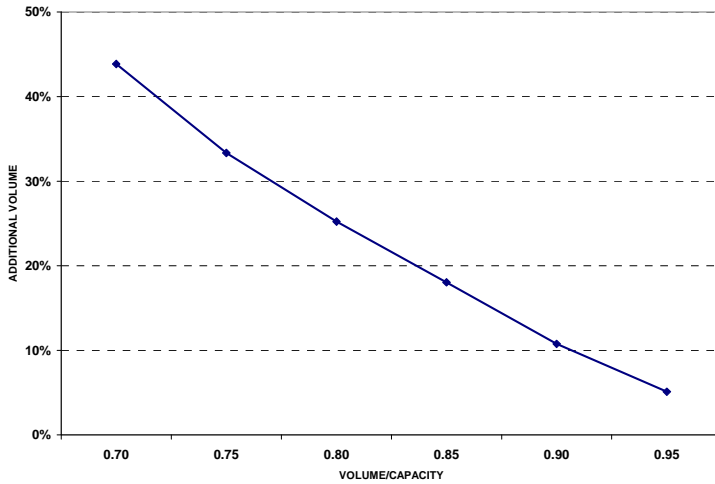
Figure 4.9 Maximum Diverted Volume vs. Critical Intersection V/c Ratio
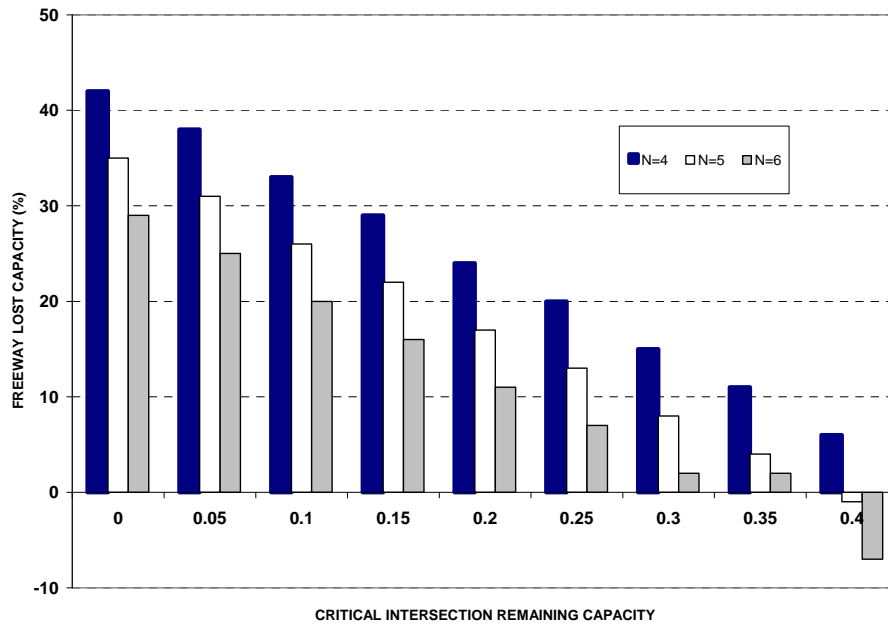
*N: number of freeway travel lanes per direction

Figure 4.10 Freeway Lost capacity vs. Critical Intersection Remaining Capacity

32

CHAPTER 5
CONCLUSIONS

Lessons learned from the application of analysis tools and strategies for management of travel corridors indicate that gaps exist in the areas of data and performance measurement, analysis tools and control strategies. This final report describes research performed on i) collection and processing of high resolution (HR) data and estimation of performance measures at signalized intersections, ii) application of analysis tools, and iii) the development and evaluation of freeway-arterial coordination strategies.

5.1 Summary of the Study Findings

HR data: We collected data on vehicle arrivals and departures plus the signal status at a real-world intersection. The processing of the data provides an extensive set of metrics that can be used for the development and assessment of signal settings at signalized intersections. The data include turning movement counts at various time resolutions, saturation flows and lost times, wasted green times, proportion of vehicles arriving on green, and delays. An algorithm was developed to estimate queue lengths from the field data.

A clustering algorithm was applied to determine the traffic demands input for developing time of day signal timing plans. The new timing plans based on the measured demands and their variations outperformed the conventional time-of-day plans based on predetermined time periods.

Application of analysis tools: a microscopic simulation model pointQ under development at UC Berkeley was independently applied and evaluated on two sites: an isolated signalized intersection and a ten intersection signalized arterial. The model predictions were compared with the output of the widely used SYNCHRO signal timing analysis and optimization software. The results indicate that the two models are in reasonably close agreement based on travel times and queue lengths. PointQ at its current state of development requires significant effort in application and cannot directly model certain operating conditions. However, it is microscopic and can be used to track individual vehicles with different O-D patterns which is a desirable feature in modeling traveler information systems.

Freeway-arterial coordination: an algorithm was developed to adjust the signal settings at intersections adjacent to freeway onramps to avoid overflow on metered on-ramps that may override the ramp metering rates. The algorithm was tested with a microscopic simulation model on a section of the I-680 freeway in the San Francisco Bay Area. The results indicate that at this particular site, the algorithm was effective in eliminating the override with significant freeway benefits and modest dis-benefits to the on-ramp traffic.

An analysis framework was developed to provide planning level estimates of the freeway volumes that can be diverted to adjacent arterial facilities given the available capacity at the critical intersection on the arterial, and how this affects the reduced freeway capacity due to an incident. This approach provides guidance for selecting candidate facilities for possible diversions and estimates of associated impacts.

5.2 Future Research

HR data: The availability of HR data at signalized intersections provides the opportunity to develop performance based signal timing plans. Instead of the traditional approach of collecting turning movement counts and use a signal optimization software to improve timing plans every few years (Figure 5.1 (a)), the performance of the intersection is continually assessed and signal control improvements can be made in a timely and effective way (Figure 5.1 (b)).

Field data collection turning movement counts	Assess existing traffic performance *Progression (% arrival on green)* *Capacity (V/c ratio)*
Develop timing plans with optimization software	Update Signal Settings
Field Implementation -fine tuning	Evaluate traffic performance

a) Traditional Approach **b) Availability of HR Data**
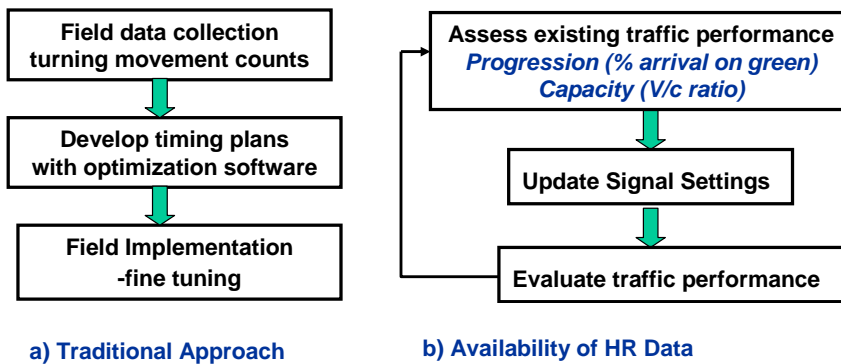
Figure 5.1 Process for Improving Signal Timing Plans

There is a need to develop systematic guidelines and analysis/optimization tools that take advantage of the availability of HR detector data. These may include flow prediction and clustering algorithms for determining timing plans, and optimal times to switch time of day plans. Also, new algorithms are needed for optimizing signal offsets based on the available data on vehicle arrivals on green.

Regarding the estimation of performance measures, there is a need to validate the queue estimation algorithm with field data (e.g., video recordings). Also, it would be of interest to compare the algorithm predictions with estimates based on emerging data sources such as connected vehicles (CV) [7,9].

Arterial analysis tools: a number of possible enhancements were identified during the application of the pointQ simulation model on real world data sets. Examples include improved modeling of traffic on intersection approaches with shared lanes and moving in several non- consecutive phases. Also it is suggested to perform a field validation of the model using readily available field data such us travel times from commercial sources and Bluetooth readers. It is also recommended a direct interface with a signal optimization tool; the existing interface with the *max pressure* algorithm requires improvements for user application.

Freeway-arterial coordination: the algorithm for preventing queue override needs to be field tested. Also, there is a need to investigate based on field measurements, the possible relationship between queue override and capacity drop at the freeway merge bottlenecks.

Additional theoretical development supplemented with simulation verification is needed for determining diversion rates in case of incidents and possible mitigation of adverse impacts on the adjacent surface street network.

REFERENCES

1. National Traffic Operations Coalition. 2012 National Traffic Report Card, 2012. http://www. ite.org/reportcard/
2. Stevanovic, A., "Adaptive Traffic Control Systems: Domestic and Foreign State of Practice," NCHRP Synthesis 403, Washington DC, 2010.
3. C.M. Day, D.M. Bullock, et al. "Performance measures for traffic signal systems: An outcome-oriented approach'" Purdue University, West Lafayette, IN, 2014, doi: 10.5703/1288284315333.
4. FHWA. "Measures of Effectiveness and Validation Guidance for Adaptive Signal Control Technologies," http://www.ops.fhwa.dot.gov/publications/fhwahop13031/index.htm
5. Skabardonis A., "Field Testing the Effectiveness of Adaptive Signal Control for Arterial Signal Management," PATH Research Report UCB-ITS-2014-3, March 2013.
6. Muralidharan, A., C. Flores, and P. Varaiya," High-Resolution Sensing of Urban Traffic," 17th IEEE ITSC Conference, Qingdao, China, October 2014.
7. Argote, J., E. Christofa and A. Skabardonis, "Connected Vehicle Penetration Rate for Estimation of Arterial Measures of Effectiveness," Transportation Research C, Vol. 60, pp. 298-312, 2015.
8. Su, D., X. Lu and R. Horowitz, "Integrating Freeway Ramp Metering and Intersection Signal Control," paper presented at the 93rd TRB Annual Meeting, Washington DC, January 2014.
9. Skabardonis, A. et al, "Advanced Traffic Signal Control Algorithms," PATH Research Report UCB-ITS-2014-4, April 2014.
10. Transportation Research Board, "Highway Capacity Manual," National Academy of Sciences, Washington DC, 2010.
11. TrafficWare, "SYNCHRO Traffic Simulation and Optimization Software, 2012.
12. Dowling , R., and S. Asiabor, "Traffic Signal Analysis with Varying Demands and Capacities," Final Report NCHRP Project 03-97, Transportaion Research Board, 2012.
13. J. Lioris, A.A. Kurzhanskiy, D. Triantafyllos and P. Varaiya. Control experiments for a network of signalized intersections using the '.Q' simulator, WODES 2014: 12th IFAC International Workshop on Discrete Event Systems, May 14-16, 2014.
14. FHWA, "Next Generation Simulation (NGSIM)," Washington DC, 2007.
15. P. Varaiya. Max Pressure control of a network of signalized intersections, Transportation Research C, 36: 177-195, 2013.
16. US DOT ITS Joint Program Office, "Integrated Corridor Management," http://www.its.dot.gov/icms/,
17. FHWA, "Coordinated freeway and arterial operations handbook". Publication No. FHWA-HRT-06-095. 2006.
18. Diakaki, C. and Papageorgiou, M. and McLean, T. "Integrated traffic-responsive urban corridor control strategy in Glasgow, Scotland". Transportation Research Record 1727, 2000.
19. Recker, W., *Development of an Adaptive Corridor Traffic Control Model*, California PATH Research Report, UCB-ITS-PRR-2008-22.
20. Zhang, H. M., J. Ma, and Y. Nie. Local Synchronization Control Scheme for Congested Interchange Areas in Freeway Corridor. *Transportation Research Record #* 2128, TRB, Washington, D.C., 2009, pp: 173-183.
21. Kwon, E., R. Ambadipudi, J. Bieniek. Adaptive Coordination of Ramp Meter and Intersection Signal for Optimal Management of Freeway Corridor, *the 82th Annual Meeting of Transportation Board*, 2003, Washington DC.
22. Tian, Z. Modeling and Implementation of an Integrated Ramp Metering – Diamond Interchange Control System. *Journal of Transportation Systems Engineering and Information Technology*, Vol. 7, No.1, 2007, pp: 61-72.
23. Xu, H., H. Liu, and Z. Tian. Control Delay at Signalized Diamond Interchanges Considering Internal Queue Spillback. Transportation Research Record #*2173*, TRB, Washington, D.C., 2010, pp: 123-132.

24. Han, B., and R. A. Reiss. Coordinating ramp meter operation with upstream intersection traffic signal. Transportation Research Record #.*1446*, TRB, Washington, D.C., 1994, pp: 44-47.
25. Kristeleit T.P., B. Bracher, K. Bogenberger, and R. L. Berini, "Ramp Metering Algorithms and Implementations- A worldwide overview," Research Report, University of Munich, 2016.
26. Horowitz, R., A. Skabardonis, M. Zhnag, P. Varayia "Design and Evaluation of Adaptive Ramp Metering Algorithms, PATH Research Report UCB-ITS-PRR-2008-10.
27. TSS|Aimsun. http://www.aimsun.com/. Accessed on March 4, 2016.
28. Caltrans PeMS. http://pems.dot.ca.gov/. Accessed on March 4, 2016.
29. Dowling, R., A. Skabardonis, and V. Alexiadis, Traffic Analysis Toolbox Volume III: Guidelines for Applying Traffic Microsimulation Modeling Software. *Federal Highway Administration*, *Publication No. FHWA-HRT-04-038*, June 2004.

APPENDIX A.

Data set 1:

```
<
AggPerf time="1440115200" health="1">
        <Leg no="1">
                <LaneCounts laneNo="1" laneType="IB" counts="14">
                        <PhaseCounts no="2" counts="9"/>
                        <PhaseCounts no="5" counts="5"/>
                </LaneCounts>
                <LaneCounts laneNo="1" laneType="OB" counts="8">
                </LaneCounts>
                <LaneCounts laneNo="2" laneType="IB" counts="3">
                        <PhaseCounts no="2" counts="3"/>
                </LaneCounts>
                <LaneCounts laneNo="2" laneType="OB" counts="21">
                </LaneCounts>
                <LaneCounts laneNo="3" laneType="IB" counts="12">
                        <PhaseCounts no="2" counts="11"/>
                </LaneCounts>
                <DelayMeasures counts="35" arriveOnGreen="15" avgDelay="6.23"/>
                <TMcounts LT="14" RT="4" T="11"/>
        </Leg>
        <Leg no="2">
                <LaneCounts laneNo="1" laneType="IB" counts="2">
                        <PhaseCounts no="1" counts="0"/>
                        <PhaseCounts no="6" counts="2"/>
                </LaneCounts>
                <LaneCounts laneNo="1" laneType="OB" counts="18">
                </LaneCounts>
                <LaneCounts laneNo="2" laneType="IB" counts="6">
                        <PhaseCounts no="6" counts="6"/>
                </LaneCounts>
                <LaneCounts laneNo="2" laneType="OB" counts="21">
                </LaneCounts>
                <LaneCounts laneNo="3" laneType="IB" counts="11">
                        <PhaseCounts no="6" counts="11"/>
                </LaneCounts>
                <LaneCounts laneNo="4" laneType="IB" counts="33">
                        <PhaseCounts no="6" counts="18"/>
                        <PhaseCounts no="4" counts="7"/>
                </LaneCounts>
                <DelayMeasures counts="54" arriveOnGreen="33" avgDelay="6.71"/>
                <TMcounts LT="1" RT="34" T="17"/>
        </Leg>
        <Leg no="3">
                <LaneCounts laneNo="1" laneType="IB" counts="14">
                        <PhaseCounts no="4" counts="13"/>
                </LaneCounts>
                <LaneCounts laneNo="1" laneType="OB" counts="14">
                </LaneCounts>
                <LaneCounts laneNo="2" laneType="IB" counts="12">
                        <PhaseCounts no="4" counts="12"/>
                </LaneCounts>
                <LaneCounts laneNo="2" laneType="OB" counts="31">
                </LaneCounts>
                <LaneCounts laneNo="3" laneType="IB" counts="16">
                        <PhaseCounts no="4" counts="7"/>
                </LaneCounts>
                <DelayMeasures counts="31" arriveOnGreen="2" avgDelay="36.08"/>
                <TMcounts LT="25" RT="13" T="3"/>
        </Leg>
        <Leg no="4">
                <LaneCounts laneNo="1" laneType="IB" counts="3">
                        <PhaseCounts no="8" counts="3"/>
                </LaneCounts>
                <LaneCounts laneNo="1" laneType="OB" counts="9">
                </LaneCounts>
                <LaneCounts laneNo="2" laneType="IB" counts="4">
                        <PhaseCounts no="8" counts="2"/>
                </LaneCounts>
                <DelayMeasures counts="6" arriveOnGreen="1" avgDelay="36.76"/>
                <TMcounts LT="4" RT="2" T="1"/>
        </Leg>
        <PhaseTimes>
                <PhaseTime no="1" greenSec="0.00" yellowSec="0.00"/>
                <PhaseTime no="2" greenSec="160.05" yellowSec="13.91"/>
                <PhaseTime no="5" greenSec="17.21" yellowSec="6.10"/>
                <PhaseTime no="6" greenSec="131.18" yellowSec="13.91"/>
                <PhaseTime no="4" greenSec="45.39" yellowSec="17.29"/>
                <PhaseTime no="8" greenSec="29.33" yellowSec="9.61"/>
        </PhaseTimes>
</AggPerf>
```

Data Set 2:

```
<SatFlow time="1439291365.900" legno="3" laneno="1" lanetype="IB" satflow="2109.67" startupLT="3.97" queueEst="7" />
```

Data Set 3:

```
<CycleMeas time="1419984090.418" cycleTime="106.24" health="1">
        <Phases>
                <Phase no="1" maxWT="0.00" wastedGreen="0.00" greenSec="0.00" yellowSec="0.00"/>
                <Phase no="2" maxWT="0.00" wastedGreen="10.36" greenSec="78.50" yellowSec="3.95"/>
                <Phase no="5" maxWT="16.53" wastedGreen="4.06" greenSec="9.00" yellowSec="3.03"/>
                <Phase no="6" maxWT="26.88" wastedGreen="2.83" greenSec="63.79" yellowSec="3.95"/>
                <Phase no="4" maxWT="248.05" wastedGreen="1.51" greenSec="15.18" yellowSec="4.30"/>
                <Phase no="8" maxWT="0.00" wastedGreen="0.00" greenSec="0.00" yellowSec="0.00"/>
        </Phases>
        <Leg no="1">
                <LaneMeas laneNo="1" laneType="IB" counts="7" redOccTime="19.57" greenOccTime="18.25" advCounts="2"
arrOnGreen="2" avgDelay="0.00">
                        <PhaseCounts no="2" counts="4"/>
                        <PhaseCounts no="5" counts="3"/>
                </LaneMeas>
                <LaneMeas laneNo="1" laneType="OB" counts="3" redOccTime="0.00" greenOccTime="0.00" advCounts="0"
arrOnGreen="0" avgDelay="0.00">
                </LaneMeas>
                <LaneMeas laneNo="2" laneType="IB" counts="5" redOccTime="0.00" greenOccTime="1.79" advCounts="7"
arrOnGreen="7" avgDelay="0.00">
                        <PhaseCounts no="2" counts="5"/>
                </LaneMeas>
                <LaneMeas laneNo="2" laneType="OB" counts="11" redOccTime="0.00" greenOccTime="0.00" advCounts="0"
arrOnGreen="0" avgDelay="0.00">
                </LaneMeas>
                <LaneMeas laneNo="3" laneType="IB" counts="5" redOccTime="15.55" greenOccTime="1.89" advCounts="5"
arrOnGreen="4" avgDelay="2.11">
                        <PhaseCounts no="2" counts="4"/>
                </LaneMeas>
        </Leg>
        <Leg no="2">
                <LaneMeas laneNo="1" laneType="IB" counts="1" redOccTime="29.81" greenOccTime="1.27" advCounts="0"
arrOnGreen="0" avgDelay="0.00">
                        <PhaseCounts no="1" counts="0"/>
                        <PhaseCounts no="6" counts="1"/>
                </LaneMeas>
                <LaneMeas laneNo="1" laneType="OB" counts="9" redOccTime="0.00" greenOccTime="0.00" advCounts="0"
arrOnGreen="0" avgDelay="0.00">
                </LaneMeas>
                <LaneMeas laneNo="2" laneType="IB" counts="3" redOccTime="4.09" greenOccTime="3.92" advCounts="4"
arrOnGreen="4" avgDelay="0.00">
                        <PhaseCounts no="6" counts="3"/>
                </LaneMeas>
                <LaneMeas laneNo="2" laneType="OB" counts="6" redOccTime="0.00" greenOccTime="0.00" advCounts="0"
arrOnGreen="0" avgDelay="0.00">
                </LaneMeas>
                <LaneMeas laneNo="3" laneType="IB" counts="4" redOccTime="23.66" greenOccTime="4.90" advCounts="6"
arrOnGreen="3" avgDelay="5.98">
                        <PhaseCounts no="6" counts="4"/>
                </LaneMeas>
                <LaneMeas laneNo="4" laneType="IB" counts="5" redOccTime="2.80" greenOccTime="11.37" advCounts="5"
arrOnGreen="4" avgDelay="0.62">
                        <PhaseCounts no="6" counts="3"/>
                        <PhaseCounts no="4" counts="1"/>
                </LaneMeas>
        </Leg>
        <Leg no="3">
                <LaneMeas laneNo="1" laneType="IB" counts="0" redOccTime="130.29" greenOccTime="93.49" advCounts="0"
arrOnGreen="0" avgDelay="0.00">
                        <PhaseCounts no="4" counts="0"/>
                </LaneMeas>
                <LaneMeas laneNo="1" laneType="OB" counts="7" redOccTime="0.00" greenOccTime="0.00" advCounts="0"
arrOnGreen="0" avgDelay="0.00">
                </LaneMeas>
                <LaneMeas laneNo="2" laneType="IB" counts="1" redOccTime="0.00" greenOccTime="1.53" advCounts="4"
arrOnGreen="1" avgDelay="29.47">
                        <PhaseCounts no="4" counts="1"/>
                </LaneMeas>
                <LaneMeas laneNo="2" laneType="OB" counts="6" redOccTime="0.00" greenOccTime="0.00" advCounts="0"
arrOnGreen="0" avgDelay="0.00">
                </LaneMeas>
                <LaneMeas laneNo="3" laneType="IB" counts="8" redOccTime="20.43" greenOccTime="3.79" advCounts="8"
arrOnGreen="1" avgDelay="36.38">
                        <PhaseCounts no="4" counts="3"/>
                </LaneMeas>
        </Leg>
        <Leg no="4">
                <LaneMeas laneNo="1" laneType="IB" counts="0" redOccTime="17.05" greenOccTime="0.00" advCounts="1"
arrOnGreen="0" avgDelay="98.71">
                        <PhaseCounts no="8" counts="0"/>
                </LaneMeas>
                <LaneMeas laneNo="1" laneType="OB" counts="5" redOccTime="0.00" greenOccTime="0.00" advCounts="0"
arrOnGreen="0" avgDelay="0.00">
                </LaneMeas>
                <LaneMeas laneNo="2" laneType="IB" counts="2" redOccTime="84.32" greenOccTime="0.00" advCounts="0"
arrOnGreen="0" avgDelay="0.00">
                        <PhaseCounts no="8" counts="0"/>
                </LaneMeas>
        </Leg>
</CycleMeas>
```

APPENDIX B

Queue-Length Estimation Using Real-Time Traffic Data

Zahra Amini, Ramtin Pedarsani, Alexander Skabardonis, Pravin Varaiya

Abstract—We consider the problem of estimating queue-lengths at an intersection from a pair of advance and stop bar detectors that count vehicles, when these measurements are noisy and biased. The key assumption is that the stop bar measurement reveals whether the queue is empty or not. We propose a real-time queue estimation algorithm based on stochastic gradient descent. The algorithm provably learns the detector bias, and efficiently estimates the queue-length with theoretical guarantee. The algorithm is tested in a simulation and in a case study using traffic data from an intersection in Beaufort, North Carolina.

I. INTRODUCTION

Knowledge of the queue lengths at signalized intersections is used in performance evaluation and for feedback signal control. Evaluation of performance measures such as intersection delay, travel time and spillback usually requires the queue length probability distribution, which can be derived from the statistics of demand and the signal control laws. For isolated intersections the distribution may be revealed through probabilistic analysis or through simulation, see, e.g. [1], [2], [3], [4], [5], [6]. For a network of intersections one must resort to simulation to estimate the joint distribution of queue lengths. But the number of simulations needed to estimate a multi-variate queue length distribution is so large that such procedures have not been reported in the literature. Instead simulations are used to estimate measures such as average delay and travel time.

Queue-based feedback control methods are proposed for example in [7], [8], [9], [10], [11]. These methods require knowledge of queue lengths in *real time*. Since they cannot be measured directly by current detection technology, one must estimate the queue lengths based on other measurements. A simple approach is to use detector vehicle counts at the entrance to the queue (e.g. from an advance detector) and at the exit of the queue (from a stop bar detector) to construct a naive queue estimate as the cumulative difference between the flows of vehicles at the entrance and the exit. But unknown biases in detector counts and random errors make this naive estimate useless, so estimation algorithms propose alternatives. For example, [12] uses time-occupancy to estimate queues, following a relationship between occupancy and counts investigated in [13]; and [14] uses high-resolution detector measurements to estimate queue lengths by first identifying 'break points' in shockwaves predicted by the LWR theory. Future availability of accurate vehicle GPS position in real time may also be exploited for queue length estimation as suggested in [15], [16], [17]. Real time estimation of queues

Z. Amini and A. Skabardonis are with the Department of Civil and Environmental Engineering, University of California, Berkeley, CA 94720 USA email: zahraamini@berkeley.edu, dromeas@berkeley.edu

R. Pedarsani and P. Varaiya are with the Department of Electrical Engineering and Computer Sciences, University of California, Berkeley, CA 94720 USA email: ramtin@berkeley.edu, varaiya@berkeley.edu

is also needed for ramp control and poses similar problems as intersection queues. [18] compares four alternative ramp queue estimation methods based on occupancy measurements at the ramp entrance, vehicle counts at the on-ramp entrance and exit, speed measurements at the ramp entrance, and vehicle reidentification based on magnetic "signatures". A unique attribute of [18] is that the estimates are compared with video-based ground truth; most algorithms are tested via simulation.

The approach described here is close to the naive estimator, corrected by compensation for the errors from biased and noisy advance and stop bar detector counts. The bias is discovered by an online learning algorithm based on stochastic gradient descent. The method provably learns the bias, and efficiently estimates the queue length with a theoretical guarantee under a certain condition on the detectors, namely, the stop bar detector reliably indicates when there is no queue in front of it.

The rest of the paper is organized as follows. In §II the queue-length estimation problem is formulated. In §III the online algorithm is described. In §IV it is proved that the algorithm learns the detector bias. The temporal convergence of the algorithm is explored through simulation and in a case study in §V and VI. Concluding remarks are collected in §VII.

II. PROBLEM FORMULATION

Time is continuous. Let $Q(t)$, $t \geq 0$ be the queue length i.e. the number of vehicles beyond the advance detector that are stopped at the stop bar at time t. The set $\{t \mid Q(t) > 0\}$ is a union of intervals called *busy periods* $(\tau_i, \bar{\tau}_i)$, $i \geq 1$; τ_i is the beginning, $\bar{\tau}_i = \tau_i + T_i$ is the end, and T_i is the length of busy period i. More precisely, $Q(t) > 0$ if $t \in \cup_i(\tau_i, \bar{\tau}_i)$ and $Q(t) = 0$ if $t \notin \cup_i(\tau_i, \bar{\tau}_i)$. We assume that the stop bar detector indicates when $Q(t) = 0$, i.e. when $t \notin \cup_i(\tau_i, \bar{\tau}_i)$. $Q(t)$ evolves as

$$Q(t) = \begin{cases} A_n(t) - D_n(t) & t \in (\tau_n, \bar{\tau}_n), \text{ for some } n \\ 0 & t \notin \cup_n(\tau_n, \bar{\tau}_n) \end{cases}, \quad (1)$$

in which $A_n(t)$, $t \in [\tau_n, \bar{\tau}_n]$ and $D_n(t) \in [\tau_n, \bar{\tau}_n]$ are the *cumulative* arrival and departure processes of the queue in the n-th busy period. That is, $A_n(t)$ vehicles entered the queue and $D_n(t)$ vehicles departed the queue during $[\tau_n, t]$. Note that arrivals during a non-busy period are immediately served, so a vehicle arriving during $t \notin \cup_n(\tau_n, \bar{\tau}_n)$ does not face a queue. Advance detectors at the entrance and stop bar detectors at the exit of the queue measure $A_n(t)$ and $D_n(t)$, possibly with some bias or independent noise. Denote by $\hat{A}_n(t)$, $t \in [\tau_n, \bar{\tau}_n]$ the cumulative counts of the entrance detector, and by $\hat{D}_n(t)$, $t \in [\tau_n, \bar{\tau}_n]$ the cumulative counts of the exit detector. Because of detector noise and bias $\hat{A}_n(t)$ may not equal $A_n(t)$ and $\hat{D}_n(t)$ may not equal $D_n(t)$. Since the stop bar detector indicates when $Q(t) = 0$, a naive queue length estimator is

$$\hat{Q}_{\text{naive}}(t) = \begin{cases} \hat{A}_n(t) - \hat{D}_n(t) & t \in (\tau_n, \bar{\tau}_n), \text{ for some } n \\ 0 & t \notin \cup_n(\tau_n, \bar{\tau}_n). \end{cases} \quad (2)$$

This naive estimator uses the information about when the queue becomes empty only to reset its estimate to zero, and does not attempt to estimate any systematic counting error. Further, it may lead to negative estimates of the queue length.

The proposed estimation algorithm and its theoretical properties are based on the following model the detector counting processes.

$$\hat{A}_n(t) - \hat{D}_n(t)$$
$$= A_n(t) - D_n(t) + \int_{\tau_n}^{t} b(t)dt + Z_n(t - \tau_n), \ t \in [\tau_n, \bar{\tau}_n]. \tag{3}$$

Here $b(t)$ is the (possibly time-varying) systematic error or bias of the detectors' counting processes, and $Z_n(t)$ is a sequence of independent cumulative zero-mean noise random variables with $Z_n(0) = 0$. We assume that $E[Z_n^2(t)] \leq c_1 t$ for some positive constant $c_1 > 0$ for all n. To prove convergence of our proposed algorithm, it is assumed that $b(t) = b$ is fixed, but in practice $b(t)$ may change with time, and simulation results show that the proposed algorithm can track the variability of $b(t)$.

III. Queue-Length Estimation Algorithm

The estimation algorithm is based on stochastic gradient descent. We assume that $b(t) = b$. Let α_n, $n \geq 1$ be the step-size (learning rate) of algorithm that is a positive decreasing sequence with the following properties:

$$\lim_{n \to \infty} \alpha_n = 0 \tag{4}$$

$$\sum_{n=1}^{\infty} \alpha_n = \infty \tag{5}$$

$$\sum_{n=1}^{\infty} \alpha_n^2 < \infty \tag{6}$$

$$\lim_{n \to \infty} \frac{1}{n\alpha_n} < \infty. \tag{7}$$

For example, $\alpha_n = \frac{1}{n}$ satisfies the above properties. The properties for the step size are standard for stochastic approximation [19]. The intuition is that the sum of the step sizes should be unbounded so that learning does not stop, and sum of the squares of step sizes should be finite so that the cumulative error of estimation remains bounded.

The estimate is designed to be

$$\hat{Q}(t) = [\hat{A}(t) - \hat{D}(t) - \varepsilon_n t]^+,$$

wherein ε_n is the correction term for busy period n, and $[x]^+ = \max(x, 0)$. ε_n is updated to learn the bias term b. Formally, the algorithm proceeds as follows.

1) Initialize $\varepsilon_0 = 0$ and $n = 0$.
2) If $t \notin \cup_n (\tau_n, \bar{\tau}_n)$, then $\hat{Q}(t) = 0$.
3) If $t \in (\tau_n, \bar{\tau}_n)$ for some n, then $\hat{Q}(t) = [\hat{A}(t) - \hat{D}(t) - \varepsilon_n(t - \tau_n)]^+$.
4) Update the correction term at the end of the busy period: $\varepsilon_{n+1} \leftarrow \varepsilon_n + \alpha_n(\hat{A}(\bar{\tau}_n) - \hat{D}(\bar{\tau}_n) - \varepsilon_n T_n)$.
5) $n \leftarrow n + 1$. Repeat steps 2–5.

We now provide some intuition for the algorithm, which tries to learn the bias b of the naive estimator in (3). To find this

bias adaptively, we consider a correction term ε_n, $n \geq 1$ that should ideally be close to b. We update ε_n based on stochastic gradient descent that tries to solve the following offline optimization problem: $\min_\varepsilon f(\varepsilon) = \frac{1}{2}(b - \varepsilon)^2$. The solution to the optimization problem is obviously $\varepsilon^* = b$. If the optimization problem is solved by gradient descent, the update rule for ε would be

$$\varepsilon_{n+1} = \varepsilon_n - \alpha \frac{\partial}{\partial \varepsilon} f(\varepsilon) = \varepsilon_n + \alpha(b - \varepsilon),$$

in which α is the step size. To find an algorithm based on knowing when the queue is empty, we replace $b - \varepsilon$ by its (scaled) unbiased estimator $\hat{A}(\bar{\tau}_n) - \hat{D}(\bar{\tau}_n) - \varepsilon_n T_n$. Lastly, stochastic approximation theory suggests a step-size α_n that satisfies (4)–(7). Note that

$$E[\hat{A}(\bar{\tau}_n) - \hat{D}(\bar{\tau}_n) - \varepsilon_n T_n | T_n] = E[bT_n - \varepsilon_n T_n + Z_n(T_n) | T_n]$$
$$= T_n(b - \varepsilon_n).$$

The simulations and the case study presented in §V and VI are based on the described algorithm. However, for the proof of convergence, we consider a slightly modified version of the algorithm. First, we make the trivial assumption that b is bounded; that is $|b| < C$ for some constant C. Let $\mathcal{C} = [-C, C]$. We define the euclidean projection operator on set $\mathcal{C}$ as $[.]_\mathcal{C}$. Second, consider a large positive constant $0 < K < \infty$ and two constants $0 < K_1 \ll K_2 < \infty$. Define the noisy negative gradient term

$$g_n \triangleq \hat{A}(\bar{\tau}_n) - \hat{D}(\bar{\tau}_n) - \varepsilon_n T_n = bT_n - \varepsilon T_n + Z_n T_n. \tag{8}$$

We update the correction term ε_n, only when $|g_n| < K$ and $T_n \in [K_1, K_2]$. The intuitive reasons behind these merely technical assumptions are as follows. First, we update the correction term only if the busy period length is bounded so that $E[Z_n^2 T_n]$ is bounded. Second, we update the correction term only if the busy period is lower bounded by an arbitrarily small but positive constant so that learning happens after each update. Thus, the fourth step of the algorithm is modified to

$$\varepsilon_{n+1} \leftarrow [\varepsilon_n + \alpha_n g_n 1_{\{|g_n| < K, T_n \in [K_1, K_2]\}}]_\mathcal{C}, \tag{9}$$

where 1_A is the indicator of event A. The modification is done to prove that $\varepsilon_n \to b$ as $n \to \infty$ almost surely. We will later see that the constant K can be chosen essentially arbitrarily but independent of n.

IV. Main Theoretical Result

In this section, we state the main theoretical result of this paper. We first state the following assumption.

Assumption 1. *Constants K, K_1 and K_2 are chosen such that $\Pr(|g_n| < K, T_n \in [K_1, K_2]) \geq \delta > 0$ for some positive constant δ.*

Assumption 1 holds when the queue is stable and visits the empty state infinitely often, since the length of the busy period has bounded mean and variance. Further, b is bounded and the noise term $B(\bar{\tau}_n) - B(\tau_n)$ is bounded with high probability. So Assumption 1 holds if the queue clears infinitely often.

For ease of notation define the event $E_n \triangleq \{|g_n| < K, T_n \in [K_1, K_2]\}$. The main theoretical result is Theorem 1.

Theorem 1. *Under Assumption 1, the correction term ε_n updated according to Equation* (9) *converges to b almost surely.*

The rest of this section is dedicated to the proof of Theorem 1. There are two key steps. We first show that the algorithm updates often enough to be able to converge. Next we show that the cumulative stochastic estimation error present in the update is an L_2-bounded martingale. So by the martingale convergence theorem the cumulative estimation error converges and has a vanishing tail, and after some time the estimation error becomes negligible. The proof technique is similar to the one in [20], [21].

Lemma 1. *The following equality holds.*

$$\lim_{n \to \infty} \sum_{i=1}^{n} \alpha_i 1_{E_i} = \infty, \tag{10}$$

almost surely.

Proof: Consider a sample path, and let $x_i \triangleq \alpha_i 1_{E_i}$. Since $x_i \geq 0$, by the monotone convergence theorem the series $\sum_{i=1}^{n} x_i$ either converges or approaches infinity. We prove the lemma by contradiction. Suppose that

$$\lim_{n \to \infty} \sum_{i=1}^{n} x_i = c,$$

for some finite $c > 0$. Define the sequence $y_n = \frac{1}{\alpha_n}$. Then, since the sequence y_n is increasing and $y_n \to \infty$ as $n \to \infty$ due to (4), by Kronecker's lemma,

$$\lim_{n \to \infty} \frac{1}{y_n} \sum_{i=1}^{n} x_i y_i = 0.$$

Thus,

$$\lim_{n \to \infty} \frac{1}{y_n} \sum_{i=1}^{n} 1_{E_i} = 0.$$

Note that by (7), $\lim_{n \to \infty} \frac{n}{y_n} > 0$. Moreover, by Assumption 1, $\Pr(E_i) \geq \delta > 0$. Thus,

$$\lim_{n \to \infty} \inf \sum_{i=1}^{n} 1_{E_i} \geq \delta.$$

This leads to a contradiction, which completes the proof of Lemma 1. ∎

From now on we work with the probability-1 event defined in Lemma 1. Define $d_n = \frac{1}{2}(\varepsilon_n - b)^2$. Fix some $\varepsilon' > 0$. We show that there exists some $n_0(\varepsilon')$ such that for all $n \geq n_0(\varepsilon')$, we have

(i) If $d_n < \varepsilon'$, then $d_{n+1} < 3\varepsilon'$.

(ii) If $d_n \geq \varepsilon'$, then $d_{n+1} \leq d_n - \beta_n$ for some positive sequence β_n, where $\sum_{n=1}^{\infty} \beta_n = \infty$ and $\beta_n \to 0$ as $n \to \infty$.

Note that property (ii) shows that for some large enough $n_1 > n_0(\varepsilon')$, $d_n < \varepsilon'$ since $\sum_{n=1}^{\infty} \beta_n = \infty$. Further, property (i) shows that d_n remains small for $n \geq n_1$. More precisely, $d_n \leq 3\varepsilon'$ if $n \geq n_1$. Since, this is true for all $\varepsilon' > 0$, it is shown that d_n converges to 0 almost surely.

First, we upper bound d_{n+1} as follows.

$$\begin{aligned}
d_{n+1} &= \frac{1}{2}(\varepsilon_{n+1} - b)^2 \\
&= \frac{1}{2}([\varepsilon_n + \alpha_n g_n 1_{A_n}]_C - b)^2 \\
&\leq \frac{1}{2}(\varepsilon_n - b)^2 + \frac{1}{2}\alpha_n^2 K^2 + \alpha_n g_n(\varepsilon_n - b)1_{A_n} \\
&= d_n - \beta_n,
\end{aligned}$$

where $\beta_n \triangleq -\alpha_n g_n(\varepsilon_n - b)1_{E_n} - \frac{1}{2}\alpha_n^2 K^2$. We now show property (ii). First note that $\frac{1}{2}\alpha_n^2 K^2 < \infty$ by (6). Thus, we need to show that $\sum_{n=1}^{\infty} \alpha_n g_n(b - \varepsilon_n)1_{E_n} = \infty$ almost surely. We simplify the expression as follows.

$$\begin{aligned}
\alpha_n g_n(b - \varepsilon_n)&1_{\{|g_n|<K\}} \\
&= \alpha_n(bT_n + Z_n(T_n) - \varepsilon_n T_n))(b - \varepsilon_n)1_{E_n} \\
&= \alpha_n[(b - \varepsilon_n)^2 T_n + v_n(b - \varepsilon_n)]1_{E_n},
\end{aligned}$$

where $v_n \triangleq Z_n(T_n)$. Note that $E[v_{n+1}|v_1, v_2, \dots, v_n] = 0$. Thus, $w_n \triangleq \sum_{m=0}^{n} \alpha_n v_n$ is an L_2-bounded martingale that is $E(w_n^2) < \infty$, since $T_n < K_2$. Thus, by the martingale convergence theorem, v_n converges to a finite random variable. Furthermore, $|b - \varepsilon_n| < 2C$ is bounded. Thus, $\sum_{n=1}^{\infty} \alpha_n v_n(b - \varepsilon_n) < \infty$ almost surely. Now by assumption in the statement of property (ii), $d_n = \frac{1}{2}(b - \varepsilon_n)^2 > \varepsilon'$. Thus, Lemma 1, (5), and the fact that $T_n > K_1$ show that $\sum_{n=1}^{\infty} \alpha_n(b - \varepsilon_n)^2 T_n = \infty$. This proves that $\sum_{n=1}^{\infty} \beta_n = \infty$; thus, property (ii) is proved.

Proving property (i) can be shown as follows.

$$d_{n+1} = \frac{1}{2}([\varepsilon_n + \alpha_n g_n 1_{E_n}]_C - b)^2 \tag{11}$$

$$\leq \frac{1}{2}(\varepsilon_n + \alpha_n g_n 1_{E_n} - b)^2 \tag{12}$$

$$\leq 2d_n + \alpha_n^2 K^2, \tag{13}$$

where (12) is due to the fact that projection is non-expansive, and (13) is due to the following inequality: $(a + b)^2 \leq 2a^2 + 2b^2$. Thus, if $d_n \leq \varepsilon'$, for large enough n, one has $\alpha_n^2 K^2 < \varepsilon'$ by (4). This proves property (i), and completes the proof of Theorem 1. □

V. SIMULATION RESULTS

We now present simulation results to demonstrate the efficacy of our algorithm. Consider a single discrete-time queue that has Poisson arrivals with rate λ vehicles per time slot. One may suppose that each time slot is 5 seconds. We set $\lambda = 1.4$ veh/(5 sec) = 1008 veh/hr. We consider a cycle time of 12 time slots or 60 seconds with 6 time slots of green signal (30 seconds), and 6 time slots of red signal. We assume that the yellow signal interval is negligible. The service time distribution in our simulation is deterministic with service rate $\mu = 0.6$ veh/sec = 2160 veh/hr if the signal is green and $\mu = 0$ if the signal is red. Thus, the stability region of the queue is $\lambda < 1.5$.

There are 3 detectors at the queue as shown in Figure 1. Detector A counts the number of vehicles that enter the queue. Detector B counts the number of vehicles that exit the queue, and detector C observes whether the queue is empty or not. We evaluate the performance of the proposed algorithm in two cases. In the first case, we assume that
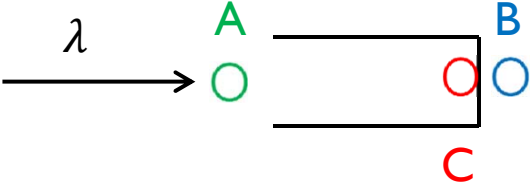
Fig. 1: A single queue equipped with 3 detectors.

detector C is noiseless, detector A counts each arriving vehicle with probability 0.95 independently, and detector B counts each departing vehicle with probability 0.85 independently. We remark that this discrete-time model is slightly different from the continuous-time model in (3); however, it captures the two important properties of the model: 1) random noise since each vehicles is observed with some probability independently, and 2) time-invariant bias since the observation probabilities of detectors A and B are different but fixed, which creates a bias. Observe that with the explained choices of the parameters, we expect to see a bias $b = (0.95 - 0.85)\lambda = 0.14$ vehicles per time slot.

In the second case, we consider 2 modes of operation: (i) the first mode is the one above; (ii) in the second mode, the arrival rate is decreased to $\lambda = 1$ veh/(5 sec) = 720 veh/hr. We assume that the system switches between these two modes every 2 hours or 1440 time slots. In this case, we choose a constant step size of $\alpha = 0.004$ so that the algorithm can adapt to the changes in the system. Note that the decaying step size enables us to prove the convergence of the correction term when b is fixed. However, when $b(t)$ is time-varying, the step size should be non-decaying so that learning does not stop. Recall that the step size is the learning rate of the algorithm. Thus, larger step size speeds up learning. However, if the step size is chosen to be too large, the gradient-descent-based algorithm may not converge.

We now evaluate the performance of the proposed algorithm in the first case. We choose the step size $\alpha_n = \frac{0.02}{n^{0.6}}$, which satisfies (4)–(7). Figure 2 shows how the correction term ε_n converges to the bias $b = 0.14$. One observes that after 30 busy periods the algorithm learns the bias and gets close to 0.14. The estimated queue-length for a period of 5000 seconds is shown in Figure 3a.

We compare the performance of our estimator with the naive estimator that does not learn the bias (though it uses the observation ;of when the queue-length is 0). We plot the cumulative distribution function (cdf) of the absolute error term in estimation that is $|Q(t) - \hat{Q}(t)|$ for the two estimators in Figure 3b. Our algorithm significantly reduces the absolute error in estimation.

Next, we consider the case that the arrival rate (thus the bias) is not constant, and it switches between two modes that have biases $b_1 = 0.14$ and $b_2 = 0.1$. Figure 4 shows how the correction term ε_n can track the changes in $b(t)$. Note that when the arrival rate is smaller, the queue empties more frequently that results in more busy periods and more learning opportunities for the algorithm.
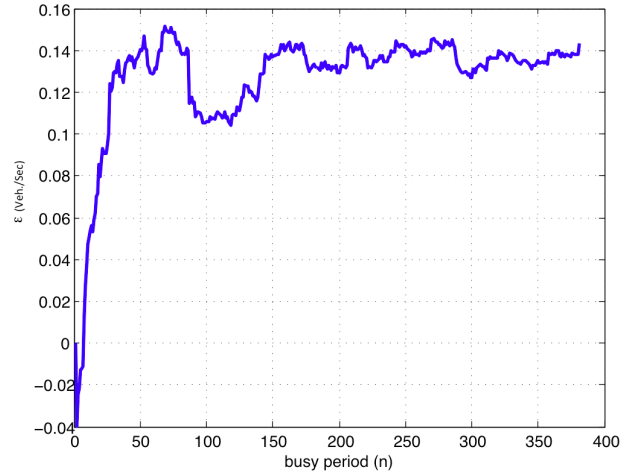

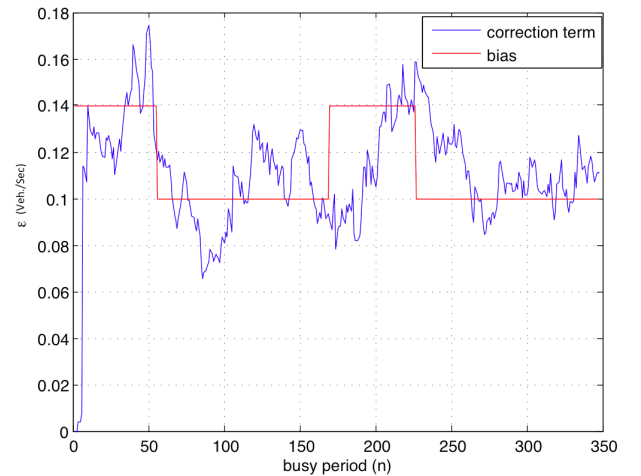Fig. 2: This figure illustrates how ε_n converges to b in a few iterations.

Fig. 4: This figure illustrates how ε_n can track the changes in the bias $b(t)$.

VI. CASE STUDY

We present a case study of an intersection in Beaufort, South Carolina. Figure 5 shows the layout of the intersection. The intersection has 4 approaches, labeled legs 1 through 4. The road is equipped with magnetic detectors from Sensys Networks, Inc (www.sensysnetorks.com). As shown in Figure 5, there are 3 types of detectors (advance, stop bar, and departure). Advance detectors are located 200-300 feet upstream of the intersection in each lane. Stop bar detectors are in front of the intersection, and detect a vehicle when it enters the intersection. Further, we have signal phase data from the controller conflict monitoring card. The measurements are time synchronous to within 0.1 sec, so we know the phase corresponding to every vehicle movement. Also available, but not used, is the time-occupancy of the sensor by each vehicle and the speed of each vehicle as it enters the intersection.

Note that the data does not include the queue length of different lanes, so there is no ground truth to evaluate
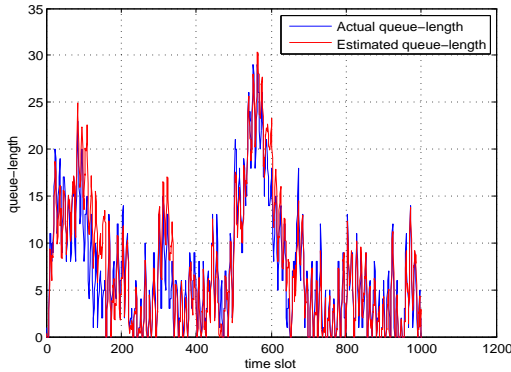
(a) Queue-length
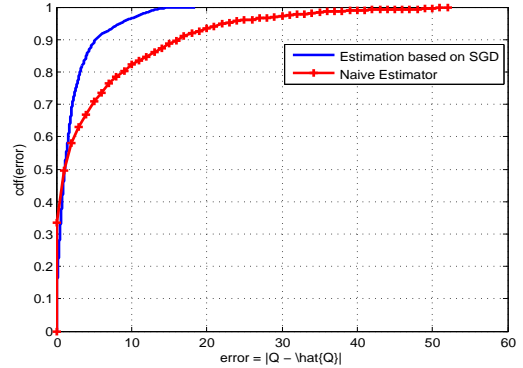
(b) CDF of absolute error

Fig. 3: Figure (a) shows the queue-length process and the estimated queue-length for 1000 time slots (5000 seconds). Figure (b) compares the absolute error in estimation for our proposed algorithm with the error of the naive estimator.

the performance of our algorithm. However, we can still investigate whether there is a bias in the detectors, and whether our algorithm can learn this bias and converge. Moreover, there is no detector that can directly measure whether the queue length is zero or not. We use the following simple rule: If the light is green and for more than 1 time slot, 3 seconds, no vehicle crosses the stop bar detector the queue is declared empty. Also, as soon as a vehicle crosses the advance detector during the red interval, a queue starts to form. It is important to mention that if a vehicle crosses both advance and stop bar detectors when there is no queue and the light is green, we do not consider that a queue of is formed. Of course, detecting whether the queue is empty or not in this way is not exact, and does not completely match the theoretical model.

We study all the legs and estimate the queue length based on observations from their advance and stop bar sensors. The time slots are of length 3 seconds. The data is for Monday May 4th, 2015, from 7:00 AM to 7:00 PM. To track the changes in the bias, we use a constant learning for the algorithm $\alpha = 0.002$.

In this period, we observe 351 busy periods spanning 354 cycles for the queue of leg 1, so the number of iterations of the gradient algorithm is 351. Figure 6 shows the evolution of the correction term ε_n. Observe that the average length of busy periods is approximately 55 seconds or 18 time slots. Figure 7 shows the queue length estimated for a 2-hour time interval, from 12:00 PM to 2:00 PM, for all legs. The reason for picking this time interval is because there are a hospital and a school close to this intersection and during lunch time, many vehicles enter the intersection resulting in large queues for the through movement.

VII. CONCLUSION AND FUTURE WORK

We considered the problem of estimating the queue lengths at an intersection from noisy and biased vehicle count observations. We developed a real-time estimation algorithm based on stochastic gradient descent that provably learns detector bias, and estimates the queue-length with theoretical guarantee. We supported our theoretical contribution with simulations results and a detailed case study.
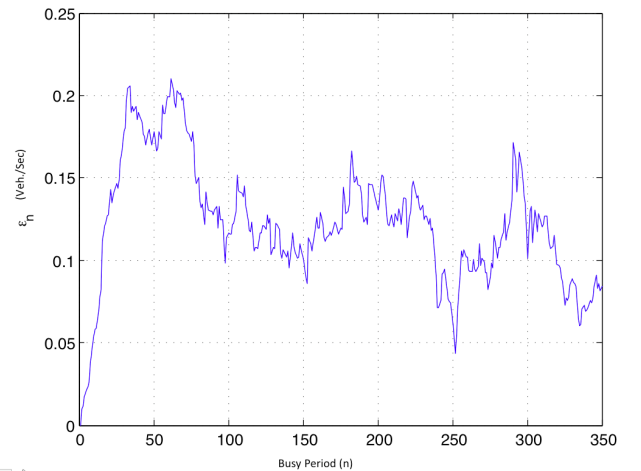

Fig. 6: The evolution of ε_n for the case study.

There are two immediate directions for future research.

- We assumed that the algorithm perfectly observes whether the queue is empty or not. It would be interesting to investigate the performance of the algorithm with noisy observation of whether the queue is empty, both theoretically and experimentally.

- One reason for estimating queue lengths is to design efficient feedback control policies for the network. For example, the max-pressure algorithm [9] is known to be throughput-optimal, but it requires knowledge of the queue lengths. An interesting question is to study the stability of the network with estimated queue lengths that are asymptotically exact. How robust is a queue based control scheme such as max-pressure to approximate queue length estimates?

REFERENCES

[1] F. V. Webster, "Traffic signal settings," Tech. Rep., 1958.
[2] A. Miller, "Settings for fixed-cycle traffic signals," *Operations Research*, vol. 14, no. 4, pp. 373–386, December 1963.
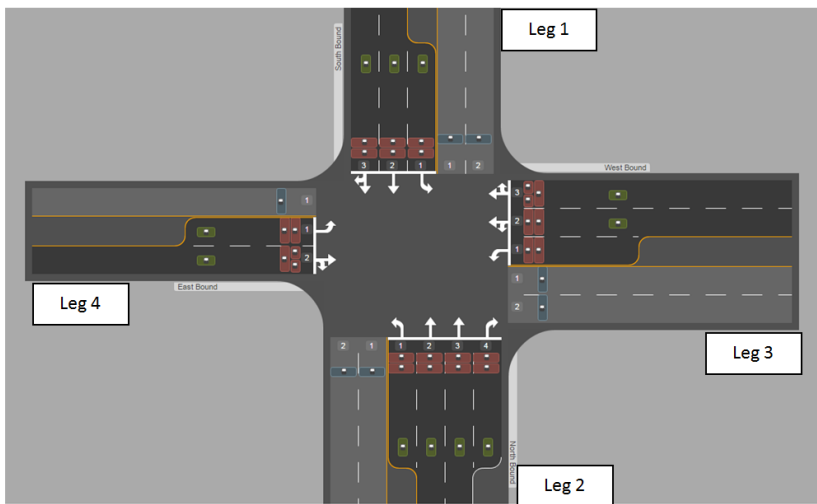
Fig. 5: Study intersection in Beaufort, NC. Each white dot is a magnetic sensor that detects when a vehicles crosses it.
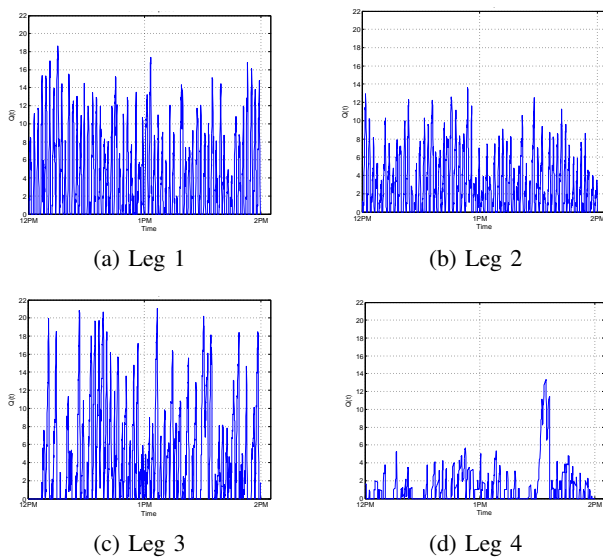

(a) Leg 1

(b) Leg 2

(c) Leg 3

(d) Leg 4

Fig. 7: Estimated queue length for all legs.

[3]   D. Heidemann, "Queue length and delay distributions at traffic signals," *Transportation Research Part B: Methodological*, vol. 28, no. 5, pp. 377–389, 1994.

[4]   G. K. Mung, A. C. Poon, and W. H. Lam, "Distributions of queue lengths at fixed time traffic signals," *Transportation Research Part B: Methodological*, vol. 30, no. 6, pp. 421–439, 1996.

[5]   F. Viti and H. J. Van Zuylen, "Probabilistic models for queues at fixed control signals," *Transportation Research Part B: Methodological*, vol. 44, no. 1, pp. 120–135, 2010.

[6]   Y. Lu and X. Yang, "Estimating dynamic queue distribution in a signalized network through a probability generating model," *Intelligent Transportation Systems, IEEE Transactions on*, vol. 15, no. 1, pp. 334–344, 2014.

[7]   P. Mirchandani and L. Head, "A real-time traffic signal control system: architecture, algorithms, and analysis," *Transportation Research, Part C*, vol. 9, pp. 415–432, 2001.

[8]   C. Diakaki, V. Dinopoulou, K. Aboudolas, M. Papageorgiou, E. Ben-Shabat, E. Seider, and A. Leibov, "Extensions and new applications of

the traffic-responsive urban control strategy," *Transportation Research Record*, vol. 1856, pp. 202–211, 2003.

[9]   P. Varaiya, "Max pressure control of a network of signalized intersections," *Transportation Research Part C: Emerging Technologies*, vol. 36, pp. 177–195, 2013.

[10]   T. Le, P. Kovács, N. Walton, H. L. Vu, L. L. Andrew, and S. S. Hoogendoorn, "Decentralized signal control for urban road networks," *Transportation Research Part C: Emerging Technologies*, 2015.

[11]   M. J. Smith, R. Liu, and R. Mounce, "Traffic control and route choice: Capacity maximisation and stability," *Transportation Research Part B: Methodological*, 2015.

[12]   K. Mucsi, A. M. Khan, and M. Ahmadi, "An adaptive neuro-fuzzy inference system for estimating the number of vehicles for queue management at signalized intersections," *Transportation Research Part C: Emerging Technologies*, vol. 19, no. 6, pp. 1033–1047, 2011.

[13]   M. Papageorgiou and G. Vigos, "Relating time-occupancy measurements to space-occupancy and link vehicle-count," *Transportation Research, Part C*, vol. 16, pp. 1–17, 2008.

[14]   H. X. Liu, X. Wu, W. Ma, and H. Hu, "Real-time queue length estimation for congested signalized intersections," *Transportation research part C: emerging technologies*, vol. 17, no. 4, pp. 412–427, 2009.

[15]   N. Geroliminis and A. Skabardonis, "Identification and analysis of queue spillovers in city street networks," *Intelligent Transportation Systems, IEEE Transactions on*, pp. 1524–9050, 2011.

[16]   M. Ramezani and N. Geroliminis, "Queue profile estimation in congested urban networks with probe data," *Computer-Aided Civil and Infrastructure Engineering*, vol. 30, no. 6, pp. 414–432, 2014.

[17]   E. Christofa, J. Argote, and A. Skabardonis, "Arterial queue spillback detection and signal control based on connected vehicle technology," *Transportation Research Record: Journal of the Transportation Research Board*, no. 2356, pp. 61–70, 2013.

[18]   R. O. Sanchez, R. Horowitz, and P. Varaiya, "Analysis of queue estimation methods using wireless magnetic sensors," *Transportation Research Record*, vol. 2229, pp. 34–45, 2011.

[19]   H. Robbins and S. Monro, "A stochastic approximation method," *The annals of mathematical statistics*, pp. 400–407, 1951.

[20]   R. Pedarsani, J. Walrand, and Y. Zhong, "Robust scheduling in a flexible fork-join network," *Decision and Control (CDC), 2014 IEEE 53rd Annual Conference on*, pp. 3669–3676, 2014.

[21]   R. Pedarsani, "Robust scheduling for queueing networks," *Ph.D. thesis*, 2015.